J. Fluid Mech. (1996), vol. 321, pp. 335 370

Upper bounds on the energy dissipation in turbulent precession

By R. R. KERSWELL†

Department of Mathematics and Statistics, University of Newcastle upon Tyne, NE1 7RU, UK

(Received 1 February 1996 and in revised form 23 April 1996)

Rigorous upper bounds on the viscous dissipation rate are identified for two commonly studied precessing fluid-filled configurations: an oblate spheroid and a long cylinder. The latter represents an interesting new application of the upper-bounding techniques developed by Howard and Busse. A novel 'background' method recently introduced by Doering & Constantin is also used to deduce in both instances an upper bound which is independent of the fluid's viscosity and the forcing precession rate. Experimental data provide some evidence that the observed viscous dissipation rate mirrors this behaviour at sufficiently high precessional forcing. Implications are then discussed for the Earth's precessional response.

1. Introduction

The enforced precession of a fluid-filled spinning container has become a popular and well-established experimental arena in which to study rotating fluids. For rapidly rotating fluids (where the Ekman number E is small), a small applied precession presents a particularly 'clean' way to excite inertial waves whether through direct forcing in the case of a spinning cylinder (Manasseh 1992, 1994; Kobine 1995) or indirectly by parametric resonance in a spinning oblate spheroid (Malkus 1968; Vanyo 1984; Vanyo *et al.* 1995). Beyond their initial excitation (Wood 1966; Kerswell 1993; Mahalov 1993), however, little is understood about how these inertial waves evolve. In particular, their tendency to suddenly and dramatically collapse to small-scale disorder still remains an elusive puzzle. Understandably, given the uncertainties surrounding this transition process, no theoretical results are as yet available to characterize the resultant precessionally forced turbulent flow. However, in many applications, such as the control of spin-stabilized projectiles or spacecraft with liquid payloads (see Selmi & Herbert 1995 for references), estimating the enhanced rate at which energy can be consumed by a precessionally stirred turbulent fluid is of fundamental concern. In this paper, we take the first steps towards supplying such an estimate by producing rigorous upper bounds on the rate of energy dissipation possible in a precessing system.

The particular emphasis here is upon obtaining upper bounds in the precessing oblate spheroidal system which serves to model the Earth's precessing outer core. A long-standing issue in geophysics has been whether the Earth's precession is an important driving agency for the complicated fluid motions thought necessary in the outer core to sustain the Earth's magnetic field against Ohmic losses. Malkus's initial suggestion (1963, 1968) envisaging a fully developed 'magnetoturbulent' flow driven

† Present address: Department of Mathematics, Bristol University, BS8 1TW, UK.

by the precessional torque was clearly motivated by his experimental hydrodynamic observations. However, the speculative nature of his accompanying arguments describing this magnetoturbulence tended to deflect attention away from the underlying idea (Rochester *et al.* 1975, see also Toomre 1966; Stacey 1973). Critiques focused upon establishing the energetic irrelevance of the *laminar* precessional response to the geodynamo (Loper 1975; Rochester *et al.* 1975) rather than considering the fully turbulent case. Here, we hope to rectify this by assessing the potency of the Earth's precession in supplying energy to the outer-core fluid. The problem considered is only the simpler hydrodynamic one for which a rigorous upper bound on the rate of viscous dissipation is derived, the hope being, of course, that this upper bound is entirely representative of the realized turbulent values. A discussion on how this dissipation is likely to be partitioned between viscous and Ohmic heating in the hydromagnetic case is, however, beyond the scope of this paper.

Upper-bounding theory represents an approach towards understanding turbulent flows without the introduction of heuristic assumptions which compromise other theories of turbulence. Formally, the underlying premise is that a fluid field becomes turbulent for a purpose which manifests itself in the maximization of some flow functional (Malkus 1954, see also Howard 1963, 1972 and Busse 1969*a*, *b*, 1970, 1978). The objective is then to identify what this functional is, i.e. what the fluid is 'trying to do', through comparing the observed turbulent field with the optimizing flow deduced from the associated variational problem for this functional. Typically, attention has been focused upon the most obvious global quantities such as heat or momentum transport since these are of immediate physical interest and can be measured experimentally. However, the search for better functional candidates remains an active area of inquiry (Ierley & Malkus 1988; Malkus & Smith 1989; Smith 1991).

Given a functional of the flow, the essential idea is then to seek an extreme of this quantity over a manifold of vector fields which satisfy only a reduced number of constraints implied by the complete set of equations. Since the realized solutions are contained within this manifold, the deduced extreme then acts to bound the observed values. The resultant bound gives a completely rigorous characterization of the turbulent flow. However, its 'closeness' to the realized values and hence utility cannot be assessed except through direct comparison with experimental measurements. In principle, this bound can be improved by incorporating further information from the governing equations in the form of additional constraints until ultimately the set of vector fields must be the solution set and the bound is attained. In practice, however, the variational problems which arise soon approach the complexity of the full system as constraints are added. The hope then is that the upper bound and the optimizing vector field may start to reflect features of the true turbulent solution before this point is reached.

Formal upper-bound theory has its origins in the work of Howard (1963) who developed the initial ideas of Malkus (1954) on turbulent convection. Howard formulated and solved the first variational problem to maximize the convective heat transport possible across a layer of fluid heated from below subject to the two dissipation rate integrals of the basic Boussinesq equations. Further developments followed, most notably through incorporating the continuity constraint into the convection problem (Busse 1969*a*) together with the subsequent application of the theory to turbulent shear flow (Busse 1969*b*, 1970, 1978), and are still continuing (Soward 1980; Howard 1990; Worthing 1995; Kerswell & Soward 1996).

Precessing systems represent an especially challenging and novel application of

upper-bound methods owing to the boundedness of the fluid and the inherent lack of symmetry of the problem. In particular, the techniques developed by Howard and Busse cannot be applied directly to the oblate spheroidal case but are instead used to advantage in a closely related cylindrical system. Nevertheless, two rigorous upper bounds on the rate of energy dissipation are derived in §2 for the oblate spheroidal system using very simple ideas from Howard (1963) and a new 'background' method recently introduced by Doering & Constantin (1992, 1994, 1996) and Constantin & Doering (1995). Since it is unknown how 'good' these bounds are, their analogues are derived in §3 for the case of a long precessing cylinder for which comparison with the powerful techniques of Howard and Busse is available. For the geophysicist interested in the Earth's precession, the technical development in §3 may be skipped with no great loss. For the applied mathematician, however, this does represent an interesting new application of the ingenious multiple boundary layer techniques pioneered by Busse. Lastly in §4, the upper-bound results are discussed in the light of experimental data and some final conclusions are drawn.

2. Bounds for a precessing oblate spheroid

Consider a fluid-filled spheroid of oblateness η spinning at an angular velocity $\omega\widehat{\boldsymbol{k}}$ about its axis of symmetry which itself is rotating at $\boldsymbol{\Omega}$ in inertial space. In the *precessing* frame, the equations are

$$\frac{\partial \boldsymbol{u}}{\partial t} + 2\boldsymbol{\Omega}\times\boldsymbol{u} + \boldsymbol{u}\cdot\nabla\boldsymbol{u} + \nabla p = E\nabla^2\boldsymbol{u}, \tag{2.1}$$

$$\nabla\cdot\boldsymbol{u} = 0, \tag{2.2}$$

$$\boldsymbol{u} = \widehat{\boldsymbol{k}}\times\boldsymbol{r}|_{\partial V}, \quad \partial V : r^2 + \eta z^2 = x^2 + y^2 + \frac{z^2}{c^2} = 1, \tag{2.3}$$

where the equatorial radius of the spheroid R, the fluid density ρ and the basic spin rate ω have been used to non-dimensionalize the system. The Ekman number E is $\nu/\omega R^2$ with ν the kinematic viscosity, and $p = P - \frac{1}{2}|\boldsymbol{\Omega}\times\boldsymbol{r}|^2$ is a modified version of the pressure P. Written in this way, the underlying spin of the fluid only appears in the tangential velocity boundary condition. As a result, it is better to work with the velocity relative to the spinning container, $\boldsymbol{u}^* = \boldsymbol{u} - \widehat{\boldsymbol{k}}\times\boldsymbol{r}$, where now the boundary conditions are homogeneous and the momentum equation (2.1) becomes

$$\left(\partial_t + \bar{\partial}_\phi\right)\boldsymbol{u}^* + 2(\boldsymbol{\Omega} + \widehat{\boldsymbol{k}})\times\boldsymbol{u}^* + \boldsymbol{u}^*\cdot\nabla\boldsymbol{u}^* + \nabla p^* - E\nabla^2\boldsymbol{u}^* = (\widehat{\boldsymbol{k}}\times\boldsymbol{\Omega})\times\boldsymbol{r}. \tag{2.4}$$

Here $\bar{\partial}_\phi = \partial_\phi - \widehat{\boldsymbol{k}}\times$ so that $\bar{\partial}_\phi$ does not act on unit base vectors and $p^* = P - \frac{1}{2}|(\boldsymbol{\Omega} + \widehat{\boldsymbol{k}})\times\boldsymbol{r}|^2$. The forcing term on the right of (2.4) has become known as the Poincaré force (Malkus 1968) and acts to drive the flow away from the uniformly spinning dissipation-free state that would otherwise be realized.

2.1. *Stokes upper bound*

It is straightforward to derive global power and torque relations. Taking $\langle \boldsymbol{u}^*\cdot(2.4)\rangle$, where $\langle\ \rangle = \int \mathrm{d}V$, and assuming a statistically steady state, gives the balance between the total viscous dissipation rate and the power input

$$\mathscr{D} := E\langle|\nabla\boldsymbol{u}^*|^2\rangle = \widehat{\boldsymbol{k}}\cdot\boldsymbol{\Omega}\times\langle\boldsymbol{r}\times\boldsymbol{u}^*\rangle \tag{2.5}$$

(no work is done in precessing the underlying flow $\hat{\boldsymbol{k}}\times\boldsymbol{r}$). An associated torque balance in the $\hat{\boldsymbol{k}}$-direction is available via $\langle\hat{\boldsymbol{k}}\cdot\boldsymbol{r}\times(2.4)\rangle$ as

$$E\langle\hat{\boldsymbol{k}}\cdot\boldsymbol{r}\times\nabla^2\boldsymbol{u}^*\rangle = \langle\hat{\boldsymbol{k}}\cdot\boldsymbol{r}\times(2\boldsymbol{\Omega}\times\boldsymbol{u}^*)\rangle = \hat{\boldsymbol{k}}\cdot\boldsymbol{\Omega}\times\langle\boldsymbol{r}\times\boldsymbol{u}^*\rangle = \hat{\boldsymbol{k}}\cdot\boldsymbol{\Omega}\times\mathscr{L}, \tag{2.6}$$

where $\mathscr{L} := \langle\boldsymbol{r}\times\boldsymbol{u}\rangle$ is the total angular momentum of the fluid. Equation (2.6) is a statement that the *working* precessional torque component exerted on the fluid by the boundary is viscously transmitted through the fluid. Modulo the spin rate (which is 1 in our non-dimensional units), this torque component equates to the dissipation rate within the fluid. Therefore, we can search for an upper bound on the energy dissipation indirectly by maximizing this torque component in the same way that bounding the heat flux leads to an estimate for the largest dissipation rate in a convecting layer of fluid (Howard 1963).

On the face of it, there are two integral relations, the continuity equation and non-slip boundary conditions with which to constrain velocity fields competing to maximize $\hat{\boldsymbol{k}}\cdot\boldsymbol{\Omega}\times\langle\boldsymbol{r}\times\boldsymbol{u}^*\rangle$. Unfortunately it is not possible to utilize the torque relation (2.6) because the viscous torque involves normal derivatives of tangential velocity components at the boundary which are unrestrained by the non-slip boundary conditions. Instead, the simplest extremal problem for the torque is to maximize the homogeneous functional

$$F(\boldsymbol{v}) = \frac{\Omega^2}{E}\frac{(\hat{\boldsymbol{k}}\cdot\hat{\boldsymbol{\Omega}}\times\langle\boldsymbol{r}\times\boldsymbol{v}\rangle)^2}{\langle|\nabla\boldsymbol{v}|^2\rangle} \tag{2.7}$$

subject to $\nabla\cdot\boldsymbol{v} = 0$ and $\boldsymbol{v} = \boldsymbol{0}$ on ∂V†. The non-slip boundary restriction is crucial: relaxing it in favour of just a vanishing normal velocity component admits the inviscid Poincaré solution (Poincaré 1910) for which the dissipation is zero. It is straightforward to demonstrate that F is bounded above so that the maximization problem is well posed. Using the Schwarz inequality,

$$\frac{E}{\Omega^2}F = \frac{\langle\boldsymbol{v}\cdot(\hat{\boldsymbol{k}}\times\hat{\boldsymbol{\Omega}})\times\boldsymbol{r}\rangle^2}{\langle|\nabla\boldsymbol{v}|^2\rangle} \leqslant \frac{\langle\boldsymbol{v}^2\rangle}{\langle|\nabla\boldsymbol{v}|^2\rangle}\langle|(\hat{\boldsymbol{k}}\times\hat{\boldsymbol{\Omega}})\times\boldsymbol{r}|^2\rangle, \tag{2.8}$$

where $\langle|(\hat{\boldsymbol{k}}\times\hat{\boldsymbol{\Omega}})\times\boldsymbol{r}|^2\rangle = \frac{4}{15}\pi c(1+c^2)$ for a spheroid $x^2+y^2+z^2/c^2 = 1$ with $\hat{\boldsymbol{\Omega}} = \hat{\boldsymbol{x}}$. (The component of the precession vector $\boldsymbol{\Omega}$ parallel to the spin axis is dynamically unimportant acting only to renormalize the basic spin rate. As a result in this paper we take $\hat{\boldsymbol{\Omega}} = \hat{\boldsymbol{x}}$ throughout.) Bounding the ratio $\lambda = \langle\boldsymbol{v}^2\rangle/\langle|\nabla\boldsymbol{v}|^2\rangle$ is a familiar situation in energy stability theory (Serrin 1959; Joseph 1976) from which (Payne & Weinberger 1963) we can borrow the result that

$$\lambda_{max}[\partial V : r^2+\eta z^2 = 1] < \lambda_{max}[\partial V : r^2 = 1] = (4.4934)^{-2}, \tag{2.9}$$

leading to the (rough) upper bound

$$F \leqslant 4.15\times10^{-2}c(1+c^2)\frac{\Omega^2}{E}. \tag{2.10}$$

This, of course, can be improved by solving the associated Euler–Lagrange problem:

$$(\hat{\boldsymbol{k}}\times\hat{\boldsymbol{\Omega}})\times\boldsymbol{r} - \nabla p + \frac{E}{\Omega^2}F\nabla^2\boldsymbol{v} = \boldsymbol{0}, \tag{2.11}$$

† The functional F depends only on the 'shape' of the velocity field and hence can be made equal to the torque by allowing (2.5) to determine the velocity amplitude.

subject to

$$\left.\begin{aligned} \langle \hat{\boldsymbol{k}}\times\hat{\boldsymbol{\Omega}}\cdot\boldsymbol{r}\times\boldsymbol{v}\rangle &= 1, \\ \nabla\cdot\boldsymbol{v} &= 0, \\ \boldsymbol{v} &= \boldsymbol{0}|_{\partial V}. \end{aligned}\right\} \tag{2.12}$$

The optimizing velocity field is easily found to be

$$\boldsymbol{v} = \frac{105}{16\pi c}\left(1 - x^2 - y^2 - \frac{z^2}{c^2}\right)\begin{bmatrix} z/c^2 \\ 0 \\ -x \end{bmatrix}, \quad p = 0, \tag{2.13}$$

giving now the best bound to (2.7) as

$$F_{max} = \frac{16\pi c^5}{105(4c^4 + 3c^2 + 3)}\frac{\Omega^2}{E}. \tag{2.14}$$

It is worth remarking that the solution (2.13) has $\langle \hat{\boldsymbol{k}}\cdot\boldsymbol{r}\times\nabla^2\boldsymbol{v}\rangle = \oint \hat{\boldsymbol{k}}\times\boldsymbol{r}\cdot(\hat{\boldsymbol{n}}\cdot\nabla)\boldsymbol{v}\,\mathrm{d}S = 0$ violating the torque constraint (2.6). However, this is of no consequence because we may adjust the torque by adding a discontinuity in $\hat{\boldsymbol{n}}\cdot\nabla v_\phi$ to $\boldsymbol{v}$ at the boundary with no penalty to F.

Actually, the optimal problem (2.11) and (2.12) is none other than a Stokes problem in the sense that all the inertial terms have been dropped from (2.4) ($\boldsymbol{u}^* = F\boldsymbol{v}/\Omega$, $p^* = \Omega p$). This is presumably the Stokes problem solved by Busse in the spherical case according to Vanyo (e.g. 1991, equation [11]) who quotes a dissipation which is exactly F_{max} for $c = 1$. Retention of the Poincaré 'forcing' term means that that there is no accompanying minimum dissipation theorem associated with this flow. Rather curiously, we have established precisely the opposite – this Stokes flow *maximizes* the dissipation. Unfortunately, the Stokes problem,

$$\left.\begin{aligned} \nabla p &= E\nabla^2\boldsymbol{v}, \\ \nabla\cdot\boldsymbol{v} &= 0, \\ \boldsymbol{v} &= \hat{\boldsymbol{k}}\times\boldsymbol{r}|_{\partial V}, \end{aligned}\right\} \tag{2.15}$$

is not particularly useful, admitting the rigid rotation solution $\boldsymbol{v} = \hat{\boldsymbol{k}}\times\boldsymbol{r}$ and hence supplying only a trivial lower bound on the dissipation rate.

2.2. *Hydromagnetic precession*

The result (2.14) may be used to derive a simple upper bound on the Ohmic dissipation rate possible in an electrically conducting fluid undergoing forced precession. The hydromagnetic analogue of the momentum equation (2.4) is

$$(\partial_t + \bar{\partial}_\phi)\,\boldsymbol{u}^* + 2(\boldsymbol{\Omega}+\hat{\boldsymbol{k}})\times\boldsymbol{u}^* + \boldsymbol{u}^*\cdot\nabla\boldsymbol{u}^* + \boldsymbol{H}\times(\nabla\times\boldsymbol{H}) + \nabla p^* - E\nabla^2\boldsymbol{u}^* = (\hat{\boldsymbol{k}}\times\boldsymbol{\Omega})\times\boldsymbol{r} \tag{2.16}$$

where the magnetic field $\boldsymbol{B} = \omega R(\rho/\mu)^{1/2}\,\boldsymbol{H}$ (ρ is density and μ the magnetic permeability), and the induction equation is

$$\frac{\partial \boldsymbol{H}}{\partial t} = \nabla\times(\boldsymbol{u}^*\times\boldsymbol{H}) + E_m\nabla^2\boldsymbol{H} \tag{2.17}$$

where E_m is the magnetic Ekman number. These yield two power integrals for a statistically steady state:

$$E\langle|\nabla\boldsymbol{u}^*|^2\rangle = \langle\boldsymbol{u}^*\cdot(\hat{\boldsymbol{k}}\times\boldsymbol{\Omega})\times\boldsymbol{r}\rangle - \langle\boldsymbol{u}^*\cdot\boldsymbol{H}\times(\nabla\times\boldsymbol{H})\rangle, \tag{2.18}$$

$$E_m\langle|\nabla\times\boldsymbol{H}|^2\rangle = \langle\boldsymbol{u}^*\cdot\boldsymbol{H}\times(\nabla\times\boldsymbol{H})\rangle, \tag{2.19}$$

with their sum describing the total power balance. The upper bound F_{max} on the torque still acts to constrain the viscous dissipation although, with Ohmic dissipation to accommodate, it becomes less sharp. We can bound the Ohmic dissipation rate quite simply by considering the homogeneous functional

$$D(\boldsymbol{v},\mathscr{H}) = \langle \boldsymbol{v}\cdot(\hat{\boldsymbol{k}}\times\boldsymbol{\Omega})\times\boldsymbol{r}\rangle \frac{E_m\langle|\nabla\times\mathscr{H}|^2\rangle}{\langle \boldsymbol{v}\cdot\mathscr{H}\times(\nabla\times\mathscr{H})\rangle} - E\langle|\nabla\boldsymbol{v}|^2\rangle \frac{E_m^2\langle|\nabla\times\mathscr{H}|^2\rangle^2}{\langle \boldsymbol{v}\cdot\mathscr{H}\times(\nabla\times\mathscr{H})\rangle^2}. \tag{2.20}$$

By choosing the amplitudes of $\boldsymbol{v}$ and $\mathscr{H}$ to satisfy each of the power relations, D is then precisely the Ohmic dissipation rate (Kennett 1974 has previously used this technique to bound Ohmic dissipation in convectively driven flows: see also Proctor 1979). Defining

$$\alpha = \frac{E_m\langle|\nabla\boldsymbol{v}|^2\rangle^{1/2}\langle|\nabla\times\mathscr{H}|^2\rangle}{\langle \boldsymbol{v}\cdot\mathscr{H}\times(\nabla\times\mathscr{H})\rangle},$$

simplifies the functional to

$$D = \frac{\langle \boldsymbol{v}\cdot(\hat{\boldsymbol{k}}\times\boldsymbol{\Omega})\times\boldsymbol{r}\rangle}{\langle|\nabla\boldsymbol{v}|^2\rangle^{1/2}}\alpha - E\alpha^2. \tag{2.21}$$

Using (2.14), and maximizing over α leads to the upper bound on the Ohmic dissipation rate

$$E_m\langle|\nabla\times\boldsymbol{H}|^2\rangle \leqslant \tfrac{1}{4}F_{max}. \tag{2.22}$$

2.3. *Possible extensions*

In convection (Howard 1963; Busse 1969*a*) and shear flow (Busse 1970, 1978; Howard 1972) optimization problems, the standard way to proceed is to identify a spatial averaging procedure under which the dependent fields may plausibly be assumed statistically steady. Invariably, these mean fields are assumed unidimensional and, in the case of velocity, unidirectional so that the averaging procedure merely integrates over the other spatial variables. The fields, and subsequently the governing equations, are then decomposed into mean and fluctuating components, with the result that a tighter optimization problem can be produced. Such an approach is strongly dependent on the boundary conditions, however, for its success. In our precessing spheroid, experimental observations suggest that the mean flow consists of a coherent rotation of the fluid about a spin axis. For low precession rates, this spin axis is close to the spheroid's axis of symmetry but appears to move into rough alignment with the precession axis at higher 'turbulent' precession rates. Looking either to characterize the *spin-down* of the flow about the spheroid's axis or the *spin-up* about the precession axis necessitates a cylindrical averaging procedure incompatible with the oblate spheroidal boundary.

Nevertheless, the spirit of this technique does suggest a way forward. Rather than a reformulation in terms of means and fluctuations, the expected symmetries of a statistically steady flow component may be imposed as additional constraints. Given the underlying rotational nature of the flow, a reasonable starting assumption is to speculate that the total angular momentum,

$$\boldsymbol{\ell} = \oint_{\partial V} \boldsymbol{r}\times\boldsymbol{u}\,\mathrm{d}S, \qquad \partial V : r^2+\eta z^2 = R^2 \leqslant 1, \tag{2.23}$$

of an arbitrary, infinitesimally thin, spheroidal shell of fluid is statistically steady. The boundary conditions dictate that the direction of this angular momentum must

be orientated with $\widehat{\boldsymbol{k}}$, the container's spin axis, at the boundary $R = 1$. However, as R decreases away from 1, the contribution to the torque integral is maximal when $\boldsymbol{\ell}$ adjusts to align with $\widehat{\boldsymbol{k}}\times\widehat{\boldsymbol{\Omega}}$ rather than $\widehat{\boldsymbol{\Omega}}$. (Presumably, the angular momentum axis strives to be somewhere in between with the component parallel to $\widehat{\boldsymbol{\Omega}}$ probably larger to create the impression of alignment with the precession axis. This component, unfortunately, does not contribute to the torque and therefore is absent from our upper-bound problem.) Adding this plausible constraint to the problem of maximizing (2.7) leads to the Euler–Lagrange equation

$$(1+\mu)(\widehat{\boldsymbol{k}}\times\boldsymbol{\Omega})\times\boldsymbol{r}+2\mu E\nabla^2\boldsymbol{u}+\nabla p+(\boldsymbol{\lambda}\times\boldsymbol{r})\times 2(\widehat{\boldsymbol{k}}+\boldsymbol{\Omega})-u_i\nabla(\boldsymbol{\lambda}\times\boldsymbol{r})_i-\boldsymbol{u}\cdot\nabla\boldsymbol{\lambda}\times\boldsymbol{r}-E\nabla^2\boldsymbol{\lambda}\times\boldsymbol{r}=\boldsymbol{0} \tag{2.24}$$

with constraints

$$\nabla\cdot\boldsymbol{u}=0,\quad \langle\widehat{\boldsymbol{k}}\times\boldsymbol{\Omega}\cdot\boldsymbol{r}\times\boldsymbol{u}\rangle = E\langle|\nabla\boldsymbol{u}|^2\rangle, \tag{2.25}$$

$$\frac{\partial\boldsymbol{\ell}}{\partial t}=\oint_{r^2+\eta z^2=R^2}\boldsymbol{r}\times\{2(\boldsymbol{\Omega}+\widehat{\boldsymbol{k}})\times\boldsymbol{u}+\boldsymbol{u}\cdot\nabla\boldsymbol{u}-E\nabla^2\boldsymbol{u}-(\widehat{\boldsymbol{k}}\times\boldsymbol{\Omega})\times\boldsymbol{r}\}\,\mathrm{d}S=\boldsymbol{0},\quad \forall R\in(0,1], \tag{2.26}$$

and boundary conditions

$$\boldsymbol{\lambda}=\boldsymbol{u}=\boldsymbol{0}|_{r^2+\eta z^2=1}. \tag{2.27}$$

The Lagrange scalar multipliers p and μ correspond to the constraints (2.25), and the vector multiplier $\boldsymbol{\lambda}$, which is a function of the oblate spheroidal radius $R=(r^2+\eta z^2)^{1/2}$, to the angular momentum constraint (2.26). As it stands this is a formidable nonlinear problem for $(\boldsymbol{u},\boldsymbol{\lambda},\mu,p)$ which may only be simplified slightly by imposing just one component of the angular momentum constraint. The most important component is that parallel to $\widehat{\boldsymbol{k}}\times\boldsymbol{\Omega}$ since this retains the Poincaré forcing term. Unfortunately, the velocity field (2.13) remains a solution despite the constraint $\partial_t(\widehat{\boldsymbol{k}}\times\boldsymbol{\Omega}\cdot\boldsymbol{\ell})=0$ and so the upper bound (2.14) is unchanged. This degeneracy rather discourages an attack on the full problem (2.24)–(2.27).

Other approaches to generate additional constraints involve either taking higher moments or suitable projections of the governing equations. The former strategy inevitably suffers from a dearth of boundary conditions and leads to new nonlinearities in the Euler–Lagrange equations which are as yet untreatable analytically. The latter procedure is eventually equivalent to confining attention to the laminar solutions of the full steady governing equations, and thus cannot hope to capture the turbulent features of the flow.

An alternative functional-analytic method for obtaining upper bounds has recently been developed by Doering & Constantin (1992, 1994, 1996) and Constantin & Doering (1995) following on from the earlier work of Hopf (1941). The strength of this method is that it does not require an averaging procedure to be defined even though a distinction is drawn between 'background' and fluctuating velocity components. As a result, it is generally more applicable than the Howard/Busse method but is not so powerful since less information is extracted from the governing equations (see Kerswell 1996). The precessing oblate spheroid represents just one such situation where only this tool can be used.

2.4. *The background technique*

Consider the fluid velocity $\boldsymbol{u}(\boldsymbol{r},t)$, relative to the precessing frame, decomposed as $\boldsymbol{u}=\boldsymbol{U}+\boldsymbol{v}$ into a steady background flow $\boldsymbol{U}(\boldsymbol{r})$ where

$$\nabla\cdot\boldsymbol{U}=0,\quad \boldsymbol{U}=\widehat{\boldsymbol{k}}\times\boldsymbol{r}|_{\partial V}, \tag{2.28}$$

and an incompressible fluctuation field $\boldsymbol{v}(\boldsymbol{r},t)$ which then satisfies *homogeneous* boundary conditions. Inserting this decomposition into the Navier–Stokes equation, (2.1), the kinetic energy of the fluctuation $\boldsymbol{v}$ evolves according to

$$\frac{\partial}{\partial t}\langle \tfrac{1}{2}\boldsymbol{v}^2\rangle + \langle \boldsymbol{v}\cdot[2\boldsymbol{\Omega}\times\boldsymbol{U}+\boldsymbol{U}\cdot\nabla\boldsymbol{U}+\boldsymbol{v}\cdot\nabla\boldsymbol{U}]\rangle = -E\langle\nabla\boldsymbol{v}:\nabla\boldsymbol{U}\rangle - E\langle|\nabla\boldsymbol{v}|^2\rangle \tag{2.29}$$

where $\nabla\boldsymbol{v}:\nabla\boldsymbol{U}=\sum_{i,j}v_{i,j}U_{i,j}$. This cross-term may be eliminated via use of the identity

$$|\nabla\boldsymbol{u}|^2 = |\nabla\boldsymbol{U}|^2 + 2\nabla\boldsymbol{v}:\nabla\boldsymbol{U} + |\nabla\boldsymbol{v}|^2$$

and the kinetic energy derivative dropped for a statistically steady flow to give

$$E\langle|\nabla\boldsymbol{u}|^2\rangle = E\langle|\nabla\boldsymbol{U}|^2\rangle - 2\langle\boldsymbol{v}\cdot2\boldsymbol{\Omega}\times\boldsymbol{U}+\boldsymbol{v}\cdot\boldsymbol{U}\cdot\nabla\boldsymbol{U}+\boldsymbol{v}\cdot\nabla\boldsymbol{U}\cdot\boldsymbol{v}+\tfrac{1}{2}E|\nabla\boldsymbol{v}|^2\rangle. \tag{2.30}$$

Formally, the total dissipation

$$\mathscr{D} = E\langle|\nabla\boldsymbol{u}^*|^2\rangle = E\langle|\nabla\boldsymbol{u}|^2\rangle - \left\{E\oint\hat{\boldsymbol{n}}\cdot\nabla\tfrac{1}{2}(\hat{\boldsymbol{k}}\times\boldsymbol{r})^2\,\mathrm{d}S = \tfrac{8}{3}\pi E\right\} \tag{2.31}$$

but as $\mathscr{D}\gg O(E)$, we can take $\mathscr{D}$ as effectively equal to $E\langle|\nabla\boldsymbol{u}|^2\rangle$. Now, if a *trial* background field $\boldsymbol{U}$ can be chosen, subject to the conditions (2.28), such that

$$\inf_{\substack{\nabla\cdot\boldsymbol{v}=0\\ \boldsymbol{v}=\boldsymbol{0}\text{ on }\partial V}} \mathscr{G}(\boldsymbol{v},\boldsymbol{U}) = \langle\boldsymbol{v}\cdot2\boldsymbol{\Omega}\times\boldsymbol{U}+\boldsymbol{v}\cdot\boldsymbol{U}\cdot\nabla\boldsymbol{U}+\boldsymbol{v}\cdot\nabla\boldsymbol{U}\cdot\boldsymbol{v}+\tfrac{1}{2}E|\nabla\boldsymbol{v}|^2\rangle \tag{2.32}$$

exists, then (2.30) furnishes an upper bound on the total dissipation rate $E\langle|\nabla\boldsymbol{u}|^2\rangle$ – Doering & Constantin (1992, 1994) refer to the restriction imposed by the existence of (2.32) as the 'spectral constraint' on $\boldsymbol{U}$. The technical challenge is then to manufacture a functional form for $\boldsymbol{U}$ which satisfies the spectral constraint *and* optimizes the upper-bound estimate available using (2.30). If $\boldsymbol{V}$ solves the associated Euler–Lagrange equations for (2.32), then

$$2(\nabla\boldsymbol{U})_{sym}\cdot\boldsymbol{V} + \nabla P - E\nabla^2\boldsymbol{V} = -2\boldsymbol{\Omega}\times\boldsymbol{U} - \boldsymbol{U}\cdot\nabla\boldsymbol{U}, \tag{2.33}$$

and the upper bound given by (2.30) can then be written as

$$E\langle|\nabla\boldsymbol{u}|^2\rangle \leqslant E\langle|\nabla\boldsymbol{U}|^2\rangle + \langle\boldsymbol{U}\cdot\nabla\boldsymbol{V}\cdot\boldsymbol{U}\rangle - \langle\boldsymbol{V}\cdot2\boldsymbol{\Omega}\times\boldsymbol{U}\rangle. \tag{2.34}$$

This is the rotational analogue of Doering & Constantin's (1994) equation (2.28).

2.5. *An upper bound*

For the spheroid $r^2+\eta z^2=1$ we define the change of variables

$$\varpi = r\left(1+\eta\cos^2\theta\right)^{1/2},\quad \vartheta=\theta$$

in the meridional plane and choose a trial background $\boldsymbol{U}=f(\varpi)\hat{\boldsymbol{k}}\times\boldsymbol{r}$ with

$$f(\varpi)=\varpi^{1/\delta} \tag{2.35}$$

where the boundary layer thickness δ is selected to ensure that the spectral constraint is satisfied. This simple choice for f appears close to the optimal one-dimensional profile: see Appendix A. In the absence of any constraint on the amplitude of $\boldsymbol{v}$, $\mathscr{G}$ will have a global minimum if and only if $2(\nabla\boldsymbol{U})_{sym}-E\nabla^2$ is a positive semi-definite operator. This reduces to requiring

$$\tfrac{1}{2}E\langle|\nabla\boldsymbol{v}|^2\rangle \geqslant |\langle\boldsymbol{v}\cdot\nabla\boldsymbol{U}\cdot\boldsymbol{v}\rangle| = |\langle(\boldsymbol{v}\cdot\hat{\boldsymbol{k}}\times\boldsymbol{r})(\boldsymbol{v}\cdot\nabla f)\rangle|. \tag{2.36}$$

We can derive a sufficient condition on δ for this to hold using simple functional arguments. Application of the fundamental theorem of calculus to the right-hand-side integral,

$$|\langle(\boldsymbol{v}\cdot\hat{\boldsymbol{k}}\times\boldsymbol{r})(\boldsymbol{v}\cdot\nabla f\rangle| \leqslant \left\langle \varpi\frac{\mathrm{d}f}{\mathrm{d}\varpi}\int_1^{\varpi}\varpi'|v_{\phi,\varpi}|\,\mathrm{d}\varpi'\int_1^{\varpi}\varpi'|v_{\varpi,\varpi}|\,\mathrm{d}\varpi'\right\rangle, \tag{2.37}$$

and then the Schwarz inequality, gives

$$\begin{aligned}|\langle(\boldsymbol{v}\cdot\hat{\boldsymbol{k}}\times\boldsymbol{r})(\boldsymbol{v}\cdot\nabla f\rangle| &\leqslant \left\langle \varpi(1-\varpi)\left|\frac{\mathrm{d}f}{\mathrm{d}\varpi}\right|\left[\int_0^1\varpi^2v_{\phi,\varpi}^2\mathrm{d}\varpi\right]^{1/2}\left[\int_0^1\varpi^2v_{\varpi,\varpi}^2\mathrm{d}\varpi\right]^{1/2}\right\rangle\\ &\leqslant \tfrac{1}{2}\delta\left\langle\frac{1}{1+\eta\cos^2\theta}v_{\phi,r}^2+\left[1+\frac{\eta\cos\theta\sin\theta}{1+\eta\cos^2\theta}\right]v_{r,r}^2+\frac{\eta\sin 2\theta}{1+\eta\cos^2\theta}v_{\theta,r}^2\right\rangle\\ &\leqslant \tfrac{1}{2}\delta\left[1+\frac{\eta}{2(1+\eta)^{1/2}}\right]\langle|\nabla\boldsymbol{v}|^2\rangle\end{aligned} \tag{2.38}$$

where we have concentrated upon the case of oblateness $\eta \geqslant 0$ in reaching the last line.† Choosing $(1+\eta/(2(1+\eta)^{1/2})\delta = \delta^* < E$ guarantees that the viscous dissipation overcomes the quadratic driving term and therefore that $\mathscr{G}(\boldsymbol{v},\boldsymbol{U})$ can be bounded from below. To estimate this minimum, we need to bound the two linear terms in $\mathscr{G}$ which is accomplished quite simply as follows:

$$\begin{aligned}|\langle\boldsymbol{v}\cdot 2\boldsymbol{\Omega}\times\boldsymbol{U}\rangle| = |\langle 2\Omega s\cos\phi f v_z\rangle| &\leqslant 2\Omega\left\langle\varpi f\int_1^{\varpi}|v_{z,\varpi}|\,\mathrm{d}\xi\right\rangle\\ &\leqslant 2\Omega\int_0^1\varpi f\,\mathrm{d}\varpi\,\langle|v_{z,\varpi}|\rangle\\ &\leqslant 2\Omega\delta\,\langle 1^2\rangle^{1/2}\langle|\nabla\boldsymbol{v}|^2\rangle^{1/2},\end{aligned} \tag{2.39}$$

and similarly

$$|\langle\boldsymbol{v}\cdot\boldsymbol{U}\cdot\nabla\boldsymbol{U}\rangle| = |\langle sf^2v_s\rangle| \leqslant \tfrac{1}{2}\delta\langle 1^2\rangle^{1/2}\langle|\nabla\boldsymbol{v}|^2\rangle^{1/2}. \tag{2.40}$$

We then have

$$\mathscr{G} \geqslant \tfrac{1}{2}(E-\delta^*)\langle|\nabla\boldsymbol{v}|^2\rangle - (2\Omega+\tfrac{1}{2})\,\delta\langle 1^2\rangle^{1/2}\langle|\nabla\boldsymbol{v}|^2\rangle^{1/2} \geqslant \frac{-(4\Omega+1)^2\langle 1^2\rangle\delta^2}{8(E-\delta^*)} \tag{2.41}$$

so that $\mathscr{G}$ is bounded below by an $O(\delta^2/E)$ quantity provided that $\delta^* < E$. The dissipation associated with the background flow is

$$E\langle|\nabla\boldsymbol{U}|^2\rangle = \frac{4\pi E}{\delta}\int_0^1\frac{(1-x^2)\left[1+(2\eta+\eta^2)x^2\right]^{1/2}}{(1+\eta x^2)^3}\left[1-\frac{\left[1+(2\eta+\eta^2)x^2\right]^{1/2}}{2\left[1+\eta x^2\right]^{1/2}}\right]\mathrm{d}x+O(E). \tag{2.42}$$

Clearly a slight oblateness only perturbs the spherical result and henceforth we set $\eta = 0$. Taking $\delta \approx E$ means that in the rapid rotation limit where $E \ll 1$ (2.30) essentially furnishes the upper bound

$$E\langle|\nabla\boldsymbol{u}|^2\rangle \leqslant \frac{4\pi}{3}. \tag{2.43}$$

This upper bound may be tightened considerably by taking full account of the fluid's incompressibility in resolving the spectral condition beyond the comparatively

† For prolateness, replace $1+\eta/(2(1+\eta)^{1/2})$ by $1/(1+\eta)$.

conservative inequality (2.38). Improvement is achieved by relaxing the constraint on the size of δ through explicitly maximizing

$$\frac{2|\langle(\boldsymbol{v}\cdot\widehat{\boldsymbol{k}}\times\boldsymbol{r})(\boldsymbol{v}\cdot\nabla f)\rangle|}{E\langle|\nabla\boldsymbol{v}|^2\rangle} \tag{2.44}$$

over all incompressible velocity fields $\boldsymbol{v}$ which vanish at the boundary. It is sufficient to look for an axisymmetric solution

$$\boldsymbol{v}=\nabla\times[\psi(r,\theta)\widehat{\boldsymbol{\phi}}]+v(r,\theta)\widehat{\boldsymbol{\phi}} \tag{2.45}$$

to the associated Euler–Lagrange problem

$$(\widehat{\boldsymbol{k}}\times\boldsymbol{r})(\boldsymbol{v}\cdot\nabla f)+(\boldsymbol{v}\cdot\widehat{\boldsymbol{k}}\times\boldsymbol{r})\nabla f+\nabla p+E\mathscr{F}\nabla^2\boldsymbol{v}=\boldsymbol{0}, \tag{2.46}$$

$$\nabla\cdot\boldsymbol{v}=0, \quad \text{with } \boldsymbol{v}=\boldsymbol{0}|_{\partial V}.$$

Taking $\widehat{\boldsymbol{\phi}}\cdot$(2.46) and $\widehat{\boldsymbol{\phi}}\cdot\nabla\times$(2.46) leads to the equations

$$\frac{\mathrm{d}f}{\mathrm{d}r}\frac{\partial}{\partial\theta}(\psi\sin\theta)+E\mathscr{F}\mathscr{D}^2v=0, \tag{2.47}$$

$$\frac{\mathrm{d}f}{\mathrm{d}r}\frac{\partial}{\partial\theta}(v\sin\theta)+E\mathscr{F}\mathscr{D}^4\psi=0, \tag{2.48}$$

where

$$\mathscr{D}^2=\nabla^2-\frac{1}{(r\sin\theta)^2},$$

to be solved subject to the boundary conditions

$$\psi=\frac{\partial\psi}{\partial r}=v=0|_{r=1}. \tag{2.49}$$

This problem bears some resemblence to that produced by a linear stability analysis of the flow in the narrow gap between two concentric rotating spheres (Soward & Jones 1983). As a result, we can expect the maximal flow to consist of $O(1)$-aspect-ratio Taylor vortices concentrated at the equator where the shear of the 'underlying' state is largest. A full numerical solution appears to confirm this picture at moderately small E (see Appendix B) justifying use of a WKB analysis to find $\mathscr{F}$ in the asymptotic limit. Therefore we seek a solution of the form

$$v(r,\theta)=\widehat{v}(r)\cos\frac{1}{\delta}\int^{\lambda}k(\lambda)\mathrm{d}\lambda, \quad \psi(r,\theta)=\delta\widehat{\psi}(r)\sin\frac{1}{\delta}\int^{\lambda}k(\lambda)\mathrm{d}\lambda \tag{2.50}$$

where $\lambda=\theta-\pi/2$ and v has been chosen symmetric about the equator without loss of generality. Equations (2.47) and (2.48) then become

$$-\delta\frac{\mathrm{d}f}{\mathrm{d}r}k\cos\lambda\,\widehat{\psi}(r)=\frac{E\mathscr{F}}{\delta}\left(\delta^2\frac{\mathrm{d}^2}{\mathrm{d}r^2}-\frac{k^2}{r^2}\right)\widehat{v}(r), \tag{2.51}$$

$$\delta\frac{\mathrm{d}f}{\mathrm{d}r}k\cos\lambda\,\widehat{v}(r)=\frac{E\mathscr{F}}{\delta}\left(\delta^2\frac{\mathrm{d}^2}{\mathrm{d}r^2}-\frac{k^2}{r^2}\right)^2\widehat{\psi}(r) \tag{2.52}$$

to be solved subject to

$$\widehat{\psi}=\frac{\mathrm{d}\widehat{\psi}}{\mathrm{d}r}=\widehat{v}=0|_{r=1}. \tag{2.53}$$

This eigenvalue problem for $\mathscr{F}=\mathscr{F}(\lambda,k;\delta,E)$ is much more straightforward than the

corresponding linear stability eigenproblem for the Taylor number $T = T(\lambda, k, \sigma[\lambda, k])$ tackled by Soward & Jones (1983). In that case, since there is also a dependent frequency $\sigma = \sigma(\lambda, k)$ for the neutral mode, the search for minimum Taylor number T had to be broadened to look for stationary points where $T_k = T_\lambda = 0$ over complex k and λ to ensure the correct asymptotic behaviour of the solution. This, of course, is subtlety different from just finding the minimum of T over real k and λ; a distinction which proves crucial for the linear stability analysis of flow between two concentric spheres. However, here no such subtleties exist since our problem is of the 'exchange of stabilities' type ($\sigma = 0$, Chandrasekhar 1961) and so $\mathscr{F}_k = \mathscr{F}_\lambda = 0$ is achieved at the real values $\lambda = 0$ and $k \approx \pm 0.404$ for $\delta \leqslant 10^{-3.5}$. Numerical calculations down to $\delta = 10^{-4}$ (see Appendix B) indicate the asymptotic result

$$\mathscr{F}_{max} \sim 0.103 \frac{\delta}{E}. \tag{2.54}$$

The spectral constraint, $\mathscr{F} \leqslant 1$, is then still satisfied by $\delta \approx 9.7E$ and we have the improved upper bound

$$E\langle |\nabla \boldsymbol{u}|^2 \rangle \leqslant 0.137\pi = 0.43 \tag{2.55}$$

in non-dimensional units.

2.6. *Improvements*

Clearly a more judicious choice of the background field could improve the bound (2.55). For example, admitting the latitudinally dependent field $\boldsymbol{U} = f(r, \theta)\hat{\boldsymbol{k}} \times \boldsymbol{r}$ would allow the background shear to be reduced away from the equator. This should leave the spectral constraint essentially unchanged but reduce the dissipation associated with the background field. However, such an improvement can only decrease the numerical coefficient rather than adjusting the scaling-law dependence on E and Ω. The only hope to achieve the latter must be to incorporate additional constraints, the most obvious of which is the torque constraint used in §2.1.

Unfortunately, this has no effect on the spectral constraint because it can only constrain the asymmetric part of the motion. This highlights an interesting feature of this problem. Experimental observations confirm that the fluid's precessional response is essentially partitioned into an axisymmetric component forced by the spinning boundary and an asymmetric *spin-over* $e^{i\phi}$ component driven by the Poincaré force. For low 'laminar' precession rates, the flow is predominantly axisymmetric but the dissipation is almost entirely due to the small spin-over motion excited. At higher 'turbulent' precession rates when the flow has spun over completely, the axisymmetric motions are now largely confined to a turbulent boundary layer and would seem to dominate the dissipation. The bound developed here as (2.55) focuses on this latter 'turbulent' scenario whereas the torque bound of §2.1 concentrates on the asymmetric Poincaré driving. In this way, the two upper bounds are in effect mutually exclusive, serving to bound either the axisymmetric or asymmetric dissipation, but nevertheless both serve individually as rigorous results for the total dissipation.

2.7. *Comments*

In this section we have produced two rigorous upper bounds on the rate of energy dissipation possible in a precessing oblate spheroid. The simple 'Stokes' result, (2.14), which varies quadratically with the precession rate, gives the tighter bound when $\Omega \ll E^{1/2}$. Intriguingly, the 'background' upper bound, which is independent of both the precession rate and viscosity, takes over when $\Omega = O(E^{1/2})$, precisely

when the laminar Poincaré flow is thought become linearly unstable (Kerswell 1993). Malkus's (1968, figure 4) experimental observations appear to corroborate this picture remarkably well. At first glance, his graph appears roughly to indicate a quadratic-like growth of the torque (and hence dissipation) with increasing precession rate until a jump is made at $\Omega = O(E^{1/2})$ to a saturated state which is insensitive to any further increases in the precession rate.

A more in-depth discussion of the experimental data available, however, is delayed until §4. Next, in §3, our purpose is rather to assess theoretically how 'good' these bounds are likely to be through their use in a precessing cylindrical system where comparison with results derived using the more powerful Howard/Busse formalism is possible.

3. Bounds for a long precessing cylinder

Here we consider a long fluid-filled cylinder of unit radius spinning about its axis with an angular velocity $\hat{\boldsymbol{k}}$ which itself is rotating at $\boldsymbol{\Omega}$ in inertial space. As mentioned earlier, the component of the precession vector $\boldsymbol{\Omega}$ parallel to the spin axis is dynamically unimportant, serving only to renormalize the basic spin rate. As a result and without loss of generality, we take $\hat{\boldsymbol{\Omega}} = \hat{x}$. In the precessing frame and non-dimensionalizing by the radius and spin rate, the governing equations are as before, (2.1)–(2.2). By taking the cylinder as very long, the infinite-length limit can be assumed so that the boundary ∂V is just $s = 1$ in cylindrical coordinates (s, ϕ, z). Essentially, this is only a useful approximation if the resulting flow is found to be periodic in the axial coordinate and there is no net mass flux along the axis. With these two criteria satisfied as they are here, the end regions of a finite but long cylinder are subdominant to the main interior. The problem for $\boldsymbol{u}$ and p is then

$$\frac{\partial \boldsymbol{u}}{\partial t} + 2\boldsymbol{\Omega}\times\boldsymbol{u} + \boldsymbol{u}\cdot\nabla\boldsymbol{u} + \nabla p = E\nabla^2\boldsymbol{u}, \tag{3.1}$$

$$\nabla\cdot\boldsymbol{u} = 0, \tag{3.2}$$

$$\boldsymbol{u} = \hat{\boldsymbol{k}}\times\boldsymbol{r}|_{\partial V}, \quad \partial V : s = 1. \tag{3.3}$$

Again working with $\boldsymbol{u}^* = \boldsymbol{u} - \hat{\boldsymbol{k}}\times\boldsymbol{r}$ to homogenize the boundary condition, we need also to remove a centrifugal-type term from the Poincaré force, leaving it independent of the axial coordinate, to rewrite the momentum equation as

$$\left(\partial_t + \bar{\partial}_\phi\right)\boldsymbol{u}^* + 2(\boldsymbol{\Omega} + \hat{\boldsymbol{k}})\times\boldsymbol{u}^* + \boldsymbol{u}^*\cdot\nabla\boldsymbol{u}^* + \nabla p^{**} - E\nabla^2\boldsymbol{u}^* = -2\boldsymbol{\Omega}\times(\hat{\boldsymbol{k}}\times\boldsymbol{r}) \tag{3.4}$$

where $p^{**} = p - \frac{1}{2}|\hat{\boldsymbol{k}}\times\boldsymbol{r}|^2$.

3.1. *Stokes upper bound*

The power balance, $\langle \boldsymbol{u}^* \cdot (3.4)\rangle$, is

$$E\langle|\nabla\boldsymbol{u}^*|^2\rangle = \langle\hat{\boldsymbol{k}}\cdot\boldsymbol{r}\times(2\boldsymbol{\Omega}\times\boldsymbol{u}^*)\rangle = \hat{\boldsymbol{k}}\cdot\boldsymbol{\Omega}\times\langle\boldsymbol{r}\times\boldsymbol{u}^*\rangle \tag{3.5}$$

where $\langle\ \rangle$ represents the average over the infinite cylindrical volume enclosed. Proceeding as before, we can look to maximize the homogeneous functional

$$F(\boldsymbol{v}) = \frac{\Omega^2}{E}\frac{[\langle\hat{\boldsymbol{k}}\cdot\boldsymbol{r}\times(2\hat{\boldsymbol{\Omega}}\times\boldsymbol{v})\rangle]^2}{\langle|\nabla\boldsymbol{v}|^2\rangle} \tag{3.6}$$

subject to $\nabla \cdot \boldsymbol{v} = 0$ and $\boldsymbol{v} = \boldsymbol{0}$ on ∂V to derive an upper bound on the dissipation rate. The Euler–Lagrange equations are

$$2\widehat{\boldsymbol{\Omega}}\times(\widehat{\boldsymbol{k}}\times\boldsymbol{r}) - \nabla p + \frac{E}{\Omega^2}F\nabla^2\boldsymbol{v} = \boldsymbol{0}, \tag{3.7}$$

subject to

$$\left.\begin{array}{c} \langle \boldsymbol{v} \cdot 2\widehat{\boldsymbol{\Omega}}\times(\widehat{\boldsymbol{k}}\times\boldsymbol{r})\rangle = 1, \\ \nabla \cdot \boldsymbol{v} = 0, \\ \boldsymbol{v} = \boldsymbol{0}|_{\partial V}, \end{array}\right\} \tag{3.8}$$

for which the optimizing velocity field is easily found to be

$$\boldsymbol{v} = \frac{6}{\pi}s(1-s^2)\cos\phi\,\widehat{\boldsymbol{k}}, \quad p = 0 \tag{3.9}$$

giving the maximum

$$F_{max} = \frac{\pi}{24}\frac{\Omega^2}{E}. \tag{3.10}$$

3.2. *The background technique*

As before we consider the full velocity field $\boldsymbol{u}(\boldsymbol{r},t)$ in the precessing frame to be composed of a steady background field $\boldsymbol{U}(\boldsymbol{r})$ which satisfies

$$\nabla \cdot \boldsymbol{U} = 0, \quad \boldsymbol{U} = \widehat{\boldsymbol{k}}\times\boldsymbol{r}|_{\partial V}$$

and an incompressible fluctuating field $\boldsymbol{v}(\boldsymbol{r},t)$ which obeys homogeneous boundary conditions. Then, under statistically steady flow conditions

$$E\langle|\nabla\boldsymbol{u}|^2\rangle = E\langle|\nabla\boldsymbol{U}|^2\rangle - 2\mathscr{G}(\boldsymbol{v},\boldsymbol{U}) \tag{3.11}$$

where

$$\mathscr{G}(\boldsymbol{v},\boldsymbol{U}) = \langle \boldsymbol{v}\cdot 2\boldsymbol{\Omega}\times\boldsymbol{U} + \boldsymbol{v}\cdot\boldsymbol{U}\cdot\nabla\boldsymbol{U} + \boldsymbol{v}\cdot\nabla\boldsymbol{U}\cdot\boldsymbol{v} + \tfrac{1}{2}E|\nabla\boldsymbol{v}|^2\rangle. \tag{3.12}$$

Choosing the background field $\boldsymbol{U} = f(s)\widehat{\boldsymbol{k}}\times\boldsymbol{r}$ with $f(s) = s^{1/\delta}$ analogous to our spheroidal choice in §2.5 means that the results derived there can be reused here. In particular, the spectral condition which ensures that $\mathscr{G}$ is bounded below is exactly as before in the asymptotic limit of $E \ll 1$; $\delta \leqslant E/0.103$. Additionally, it follows that $\mathscr{G}_{min} = O(\delta^2/E)$ is negligible compared to the dissipation in the background field so that (3.11) effectively furnishes the upper bound

$$E\langle|\nabla\boldsymbol{u}|^2\rangle \leqslant E\langle|\nabla\boldsymbol{U}|^2\rangle = 0.103\pi = 0.32. \tag{3.13}$$

3.3. *Howard/Busse mean field formulation*

In the axially unbounded cylinder limit, a two-dimensional averaging procedure so central to the Howard/Busse approach is naturally defined for a given radius s by integration over the infinite cylinder at this radius. Armed with this, we make the very plausible and standard assumption that the averages of the velocity components and their products over cylinders of constant s (denoted by an overbar) exist and are independent of time for a statistically steady turbulent flow. We then have the mean–fluctuation decomposition

$$\boldsymbol{u}^* = \boldsymbol{u} - \widehat{\boldsymbol{k}}\times\boldsymbol{r} = V(s)\widehat{\boldsymbol{\phi}} + \boldsymbol{u}'(\boldsymbol{x},t) \tag{3.14}$$

where $\overline{\boldsymbol{u}'\cdot\hat{\boldsymbol{s}}} = \overline{\boldsymbol{u}'\cdot\hat{\boldsymbol{\phi}}} = \overline{\boldsymbol{u}'\cdot\hat{\boldsymbol{z}}} = 0$. The mean momentum equation is obtained via $\overline{\hat{\boldsymbol{\phi}}\cdot(3.4)}$ as

$$-\frac{2\Omega}{s}\overline{xu_z'} + \frac{1}{s^2}\frac{\mathrm{d}}{\mathrm{d}s}\left(s^2\overline{u_s'u_\phi'}\right) = E\left(\nabla^2 - \frac{1}{s^2}\right)V = E\frac{1}{s^2}\frac{\mathrm{d}}{\mathrm{d}s}\left[s^2\left\{s\frac{\mathrm{d}}{\mathrm{d}s}\left(\frac{V}{s}\right)\right\}\right] \tag{3.15}$$

and the fluctuation power balance, $\langle \boldsymbol{u}'\cdot(3.4)\rangle$, is

$$\left\langle \frac{2\Omega}{s}V\overline{xu_z'}\right\rangle + \left\langle \overline{su_s'u_\phi'}\frac{\mathrm{d}}{\mathrm{d}s}\left(\frac{V}{s}\right)\right\rangle + E\langle|\nabla\boldsymbol{u}'|^2\rangle = \langle -2\Omega\overline{xu_z'}\rangle \tag{3.16}$$

under the assumption of statistical steadiness and where

$$\overline{A} = \lim_{d\to\infty}\frac{1}{4\pi d}\int_{-d}^{+d}\mathrm{d}z\int_0^{2\pi}\mathrm{d}\phi\, A,$$

$$\langle A\rangle = \lim_{d\to\infty}\frac{1}{2d}\int_{-d}^{+d}\mathrm{d}z\int_0^{2\pi}\mathrm{d}\phi\int_0^1 s\,\mathrm{d}s\, A = 2\pi\int_0^1 s\,\mathrm{d}s\,\overline{A}.$$

For completeness, we note that another mean momentum statement can be made via $\overline{\hat{\boldsymbol{z}}\cdot(3.4)}$ as

$$2\Omega\left[\overline{u_s'\sin\phi + u_\phi'\cos\phi}\right] + \frac{1}{s}\frac{\mathrm{d}}{\mathrm{d}s}\left(s\overline{u_s'u_z'}\right) = 0, \tag{3.17}$$

although in what follows, this is trivially satisfied and is not considered further.

The formal upper-bound problem to be tackled is then to maximize $\mathscr{D} = \langle -2\Omega xu_z'\rangle$, the work done by the Poincaré force, subject to the constraints (3.15), (3.16), $\nabla\cdot\boldsymbol{u}' = 0$ and boundary conditions $\boldsymbol{u}'(1,\phi,z,t) = \boldsymbol{0}$, $V(1) = 0$. The global constraint linking the total dissipation, the stress at the boundary and the work done by the Poincaré force is recovered simply by taking $\langle V\times(3.15)\rangle + (3.16)$ and $\langle s\times(3.15)\rangle$,

$$\mathscr{D} = E\langle|\nabla\boldsymbol{u}^*|^2\rangle = E\langle|\nabla V|^2\rangle + E\langle|\nabla\boldsymbol{u}'|^2\rangle = 2\pi Es\frac{\mathrm{d}}{\mathrm{d}s}\left(\frac{V}{s}\right)\Big|_{s=1}.$$

In unidirectional shear flow problems (Busse 1970), an expression for the mean shear term (here $s(\mathrm{d}/\mathrm{d}s)(V/s)$) can be found in terms of the boundary stress and fluctuation Reynolds stress by integrating the mean momentum equation (3.15) once. This is then used to eliminate the mean flow completely from the fluctuation power balance, (3.16), and thereby the full optimization problem. Here, the Coriolis term prevents any such initial simplification and so we deal with the full Lagrangian

$$\begin{aligned}\mathscr{L} = \langle -2\Omega xu_z'\rangle + \mu\left\{\left\langle -2\Omega\overline{xu_z'} - \frac{2\Omega}{s}V\overline{xu_z'} - \overline{su_s'u_\phi'}\frac{\mathrm{d}}{\mathrm{d}s}\left(\frac{V}{s}\right) - E|\nabla\boldsymbol{u}'|^2\right\rangle\right\}\\ + \left\langle\lambda(s)\left\{-\frac{2\Omega}{s}\overline{xu_z'} + \frac{1}{s^2}\frac{\mathrm{d}}{\mathrm{d}s}(s^2\overline{u_s'u_\phi'}) - E\left(\nabla^2 - \frac{1}{s^2}\right)V\right\}\right\rangle - \langle 2\mu p\nabla\cdot\boldsymbol{u}'\rangle,\end{aligned} \tag{3.18}$$

where μ, p and $\lambda(s)$ are Lagrange multipliers. The Euler–Lagrange equations for $\boldsymbol{u}'$ and V are then

$$-2\Omega x\left(1+\mu+\frac{\mu V+\lambda}{s}\right)\hat{\boldsymbol{k}} - (u_s'\hat{\boldsymbol{\phi}} + u_\phi'\hat{\boldsymbol{s}})s\frac{\mathrm{d}}{\mathrm{d}s}\left(\frac{\mu V+\lambda}{s}\right) + 2\mu\nabla p + 2\mu E\nabla^2\boldsymbol{u}' = \boldsymbol{0} \tag{3.19}$$

and

$$-\mu\frac{2\Omega}{s}\overline{xu_z'} + \frac{\mu}{s^2}\frac{\mathrm{d}}{\mathrm{d}s}(s^2\overline{u_s'u_\phi'}) - E\left(\nabla^2 - \frac{1}{s^2}\right)\lambda = 0 \tag{3.20}$$

to be solved subject to

$$-\frac{2\Omega}{s}\overline{xu'_z}+\frac{1}{s^2}\frac{\mathrm{d}}{\mathrm{d}s}\left(s^2\overline{u'_s u'_\phi}\right)=E\left(\nabla^2-\frac{1}{s^2}\right)V, \tag{3.21}$$

$$\left\langle\frac{2\Omega}{s}V\overline{xu'_z}\right\rangle+\left\langle s\overline{u'_s u'_\phi}\frac{\mathrm{d}}{\mathrm{d}s}\left(\frac{V}{s}\right)\right\rangle+E\langle|\nabla\boldsymbol{u}'|^2\rangle=\langle-2\Omega\overline{xu'_z}\rangle, \tag{3.22}$$

$$\nabla\cdot\boldsymbol{u}'=0,\quad \boldsymbol{u}'(1,\phi,z,t)=\boldsymbol{0},\quad V(1)=\lambda(1)=0. \tag{3.23}$$

Subtracting (3.20) from $\mu\times$(3.22) gives

$$\left(\nabla^2-\frac{1}{s^2}\right)(\mu V-\lambda)=0 \tag{3.24}$$

which, together with the condition that $\mu V-\lambda=0$ at $s=1$ and remains regular otherwise, means that $\lambda=\mu V$. Furthermore, it is clear from the structure of $\mathscr{D}$ that $\boldsymbol{u}'$ must have the form

$$\boldsymbol{u}'=W(s)\cos\phi\,\hat{\boldsymbol{k}}+\tilde{\boldsymbol{u}}(s,\phi,z,t). \tag{3.25}$$

With this the optimization problem is now to solve

$$\Omega s\left(1+\mu+\frac{2\mu V}{s}\right)=\mu E\left(\nabla^2-\frac{1}{s^2}\right)W, \tag{3.26}$$

$$s\frac{\mathrm{d}}{\mathrm{d}s}\left(\frac{V}{s}\right)(\tilde{u}_\phi\hat{\boldsymbol{s}}+\tilde{u}_s\hat{\boldsymbol{\phi}})=\nabla p+E\nabla^2\tilde{\boldsymbol{u}}, \tag{3.27}$$

$$-\Omega W+\frac{1}{s^2}\frac{\mathrm{d}}{\mathrm{d}s}\left(s^2\overline{\tilde{u}_s\tilde{u}_\phi}\right)=E\left(\nabla^2-\frac{1}{s^2}\right)V, \tag{3.28}$$

$$\langle\, s\Omega W(\mu-1)\,\rangle=2\mu\left\langle s\overline{\tilde{u}_s\tilde{u}_\phi}\frac{\mathrm{d}}{\mathrm{d}s}\left(\frac{V}{s}\right)\right\rangle, \tag{3.29}$$

with

$$\nabla\cdot\tilde{\boldsymbol{u}}=0,\quad \tilde{\boldsymbol{u}}(1,\phi,z,t)=\boldsymbol{0},\quad W(1)=V(1)=0. \tag{3.30}$$

The key equation of this set is the mean momentum balance (3.28). This describes a three-way balance between the Poincaré forcing, the fluctuation Reynolds stress and the viscous stress in the mean flow. The first of these will only contribute in the interior away from the boundary where W must vanish, whereas the third will only be significant close to the boundary where large gradients can develop. The fluctuation Reynolds stress term then acts as an intermediary to link these interior and boundary layer regimes. Without this flexibility, the viscous boundary stress and hence the total dissipation rate will be much reduced owing to the restriction imposed by directly matching the viscous stresses with the Poincaré forcing. As an illustration, just such a scenario occurs at $\mu=1$ when a solution with vanishing fluctuation field $\tilde{\boldsymbol{u}}$ can be found. In this degenerate case, the system may be reduced to

$$2(s+V)=\epsilon^2\left(\nabla^2-\frac{1}{s^2}\right)W, \tag{3.31}$$

$$-W=\epsilon^2\left(\nabla^2-\frac{1}{s^2}\right)V \tag{3.32}$$

with $\epsilon=(E/\Omega)^{1/2}$, and $V(1)=W(1)=0$. The solution for $\epsilon\ll1$ has the boundary

layer character,

$$V = -s + \mathrm{e}^{-\xi}\cos\xi, \tag{3.33}$$

$$W = -\sqrt{2}\mathrm{e}^{-\xi}\sin\xi, \tag{3.34}$$

in terms of the stretched variable

$$\xi = \frac{1-s}{2^{1/4}\epsilon}$$

and the corresponding dissipation

$$\mathscr{D} = 2^{3/4}\pi(\Omega E)^{1/2} + O(E). \tag{3.35}$$

While this is significantly larger than the $O(\Omega^2 E^{1/2})$ laminar dissipation, it is also considerably smaller than the 'background' result independent of E or Ω derived above.

For $\mu \neq 1$, we can think in terms of the interior balance

$$\Omega s\left(1+\mu+\frac{2\mu V_i}{s}\right) = \mu E\left(\nabla^2 - \frac{1}{s^2}\right) W_i, \tag{3.36}$$

$$s\frac{\mathrm{d}}{\mathrm{d}s}\left(\frac{V_i}{s}\right)(\tilde{u}_{i\phi}\hat{\boldsymbol{s}} + \tilde{u}_{is}\hat{\boldsymbol{\phi}}) = \nabla p_i + E\nabla^2\tilde{\boldsymbol{u}}_i, \tag{3.37}$$

$$-\Omega W_i + \frac{1}{s^2}\frac{\mathrm{d}}{\mathrm{d}s}\left(s^2\overline{\tilde{u}_{is}\tilde{u}_{i\phi}}\right) = 0 \tag{3.38}$$

together with the boundary layer balance

$$s\frac{\mathrm{d}}{\mathrm{d}s}\left(\frac{V_b}{s}\right)(\tilde{u}_{b\phi}\hat{\boldsymbol{s}} + \tilde{u}_{bs}\hat{\boldsymbol{\phi}}) = \nabla p_b + E\nabla^2\tilde{\boldsymbol{u}}_b, \tag{3.39}$$

$$\frac{1}{s^2}\frac{\mathrm{d}}{\mathrm{d}s}\left(s^2\overline{\tilde{u}_{bs}\tilde{u}_{b\phi}}\right) = E\left(\nabla^2 - \frac{1}{s^2}\right)V_b, \tag{3.40}$$

and global balance

$$\langle\, s\Omega W_i(\mu-1)\,\rangle = 2\mu\left\langle s\overline{\tilde{u}_{is}\tilde{u}_{i\phi}}\frac{\mathrm{d}}{\mathrm{d}s}\left(\frac{V_i}{s}\right) + s\overline{\tilde{u}_{bs}\tilde{u}_{b\phi}}\frac{\mathrm{d}}{\mathrm{d}s}\left(\frac{V_b}{s}\right)\right\rangle, \tag{3.41}$$

where the interior flows $\tilde{\boldsymbol{u}}_i$ and V_i match smoothly onto the boundary layer flows $\tilde{\boldsymbol{u}}_b$ and V_b which then both vanish at $s = 1$. The boundary layer part W_b of W is $\ll O(W_i)$ as well as playing no significant role in either equation (3.40) or (3.41). As a result, we can apply the boundary condition $W_i(1) = 0$ and the boundary layer version of equation (3.36) which defines W_b can be neglected (see Appendix C for justification).

Integrating equation (3.40) once leads to

$$Es\frac{\mathrm{d}}{\mathrm{d}s}\left(\frac{V_b}{s}\right) = \frac{\Gamma}{s^2} + \overline{\tilde{u}_{bs}\tilde{u}_{b\phi}} \quad \text{where} \quad \Gamma = \mathscr{D}/2\pi = Es\frac{\mathrm{d}}{\mathrm{d}s}\left(\frac{V_b}{s}\right)_{s=1}. \tag{3.42}$$

The boundary layer problem (3.39) and (3.42) together with given interior boundary conditions is then exactly equivalent to finding the stationary values of the boundary layer energy dissipation

$$\mathscr{D}_{bl} = E\langle\,|\nabla\tilde{\boldsymbol{u}}_b|^2\,\rangle + \frac{\langle\,|\Gamma/s^2 + \overline{\tilde{u}_{bs}\tilde{u}_{b\phi}}|^2\,\rangle}{E} \tag{3.43}$$

for fixed Γ and $\nabla\cdot\tilde{\boldsymbol{u}}_b = 0$. This variational problem is closely related to that formulated and solved by Busse (1970) in his upper bounding of the dissipation in turbulent planar Couette flow. There the problem was to maximize the dissipation functional (3.43) across the whole planar extent of the fluid. Following his earlier success in bounding the heat transport in turbulent convection (Busse 1969*a*), Busse constructed an ingenious multi-α solution to the variational problem based upon a series of interwoven boundary layers each corresponding to a single-α spanwise wavelength. Here, we expect a similar form of solution to be relevant in our boundary layer regime but now this must be coupled to an active interior flow driven by the Poincaré force.

3.3.1. *Boundary layer regime*

Motivated by experimental observations (Townsend 1956), Busse (1970) made the assumption that the maximal fluctuating velocity solution to his Couette flow variational problem would be two-dimensional, consisting of purely streamwise rolls. In the present context, this is an assumption that the fluctuating field will be axisymmetric (Taylor–Couette rolls) which we subsequently adopt through the streamfunction representation

$$\tilde{\boldsymbol{u}}_b = \nabla\times\left[\frac{\psi(s,z)}{s}\hat{\boldsymbol{\phi}}\right] + v(s,z)\hat{\boldsymbol{\phi}}. \tag{3.44}$$

The equations to be solved in the boundary layer regime (where $s \approx 1$) are then

$$\psi_z(\Gamma - \overline{v\psi_z}) + E^2\nabla^2 v = 0, \tag{3.45}$$

$$v_z(\Gamma - \overline{v\psi_z}) + E^2\nabla^4\psi = 0 \tag{3.46}$$

with $v = \psi_s = \psi_z = 0|_{s=1}$. As mentioned earlier, these are the Euler–Lagrange equations for finding the stationary value(s) of the boundary layer dissipation

$$\mathscr{D}_{bl} = E\left\{\langle\,|\nabla\times v\hat{\boldsymbol{\phi}}|^2 + |\nabla^2\psi\hat{\boldsymbol{\phi}}|^2\,\rangle + \frac{1}{E^2}\langle\,(\Gamma - \overline{v\psi_z})^2\,\rangle\right\} \tag{3.47}$$

given that Γ, the total dissipation rate (modulo 2π), is a constant and interior boundary conditions on v, ψ_s and ψ_z. Clearly, $\mathscr{D}_{bl}$ only has a global minimum which we can use to identify a solution to the equations (3.45) and (3.46). (This is not to say that maximizing the total dissipation is achieved by minimizing the boundary layer contribution but rather that given a prescribed interior flow and fixed Γ, the boundary layer solution minimizes its dissipation.) The solution strategy is then essentially that of Busse (1969*a*, 1970). For $E \ll 1$, the mean dissipation term dominates unless $\overline{v\psi_z} \approx \Gamma$ for most of the boundary region and only then will a minimum occur when all three terms of (3.47) have the same order. The fluctuation dissipation will be minimized when the velocity gradients normal and tangential to the boundary are comparable. This suggests a sequence of boundary layers whose purpose is to gradually relax the length scales from their initial value at the boundary over which $\overline{v\psi_z} \to 0$ to a more moderate interior value.

We therefore consider the multi-α solution

$$v(s,z) = \sum_{n=1}^{N}\sqrt{2}\,v_n(s)\cos\alpha_n z, \quad \psi(s,z) = \sum_{n=1}^{N}\sqrt{2}\,\psi_n(s)\sin\alpha_n z, \tag{3.48}$$

consisting of N harmonics interwoven over N boundary layers. Formally, each harmonic occupies a triple deck of boundary layers where normal s-gradients dominate

in the innermost layer, tangential z-gradients dominate in the outermost layer and both are comparable in the intermediary layer. Fortunately, this middle layer makes no significant contribution to the optimization problem and therefore is not considered. Thus, the nth harmonic is assumed to exist only in the nth and $(n-1)$th boundary layers. In the former, inner, layer it grows from the boundary values $v_n = \psi_n = \partial\psi_n/\partial s = 0$ over a length scale of E^{r_n}. In the $(n-1)$th layer where the next harmonic v_{n-1} and ψ_{n-1} is growing, the nth harmonic v_n and ψ_n decreases to zero over the length scale $E^{r_{n-1}}$. The interaction between two overlapping harmonics in a given layer is then designed so that

$$v_{n-1}\psi_{n-1} + v_n\psi_n \approx \Gamma \tag{3.49}$$

throughout all but the innermost Nth boundary layer. Mathematically, the motivation for this design has already been given in terms of minimizing the mean flow dissipation until it is comparable to the fluctuation dissipation. Physically, this boundary layer structure may be interpreted as the mechanism by which eddies of different scale relieve one another in carrying the transport of momentum (Busse 1970).

The mathematical description must admit the fact that v and ψ may have very different orders of magnitude despite their product being $O(\Gamma)$ throughout. Certainly in the inner layer of a harmonic's triple deck where both v and ψ grow from 0, v must quickly become larger than ψ for the toroidal dissipation to be of the same order as the poloidal dissipation. Thus, the nth harmonic is rewritten as

$$\left.\begin{aligned} v_n(s) &= E^{-p_n}\hat{v}_n(\zeta_n) \\ \psi_n(s) &= E^{a+p_n+e_n}\hat{\psi}_n(\zeta_n) \end{aligned}\right\} \quad \text{for } 1-s = O(E^{r_n}),$$
$$\left.\begin{aligned} v_n(s) &= E^{-s_n}\tilde{v}_n(\zeta_{n-1}) \\ \psi_n(s) &= E^{a+s_n+e_n}\tilde{\psi}_n(\zeta_{n-1}) \end{aligned}\right\} \quad \text{for } 1-s = O(E^{r_{n-1}}) \tag{3.50}$$

where the rescaled boundary layer variables are

$$\zeta_n = (1-s)E^{-r_n}, \tag{3.51}$$

the axial wavelengths $\alpha_n = E^{-e_n}b_n$ and, most importantly, we let the as yet unknown order of the total dissipation with respect to E be a, i.e.

$$\Gamma = E^a\hat{\Gamma} \quad \text{with} \quad \hat{\Gamma} = O(1). \tag{3.52}$$

The functional $\mathscr{D}_{bl}$ is then to leading order given by

$$\begin{aligned} \mathscr{D}_{bl}/2\pi = E\sum_{n=1}^{N}\Bigg\{ & E^{-2p_n-r_n}\int_0^\infty \hat{v}_n'^2 \mathrm{d}\zeta_n + E^{2p_n+2e_n-3r_n+2a}\int_0^\infty \hat{\psi}_n''^2 \mathrm{d}\zeta_n \\ & + E^{-2s_{n+1}-2e_{n+1}+r_n} b_{n+1}^2 \int_0^\infty \tilde{v}_{n+1}^2 \mathrm{d}\zeta_n + E^{2s_{n+1}-2e_{n+1}+r_n+2a} b_{n+1}^4 \int_0^\infty \tilde{\psi}_{n+1}^2 \mathrm{d}\zeta_n \Bigg\} \\ & + \sum_{n=1}^{N} E^{2a-1+r_n}\int_0^\infty \left(\hat{\Gamma} - b_n\hat{v}_n\hat{\psi}_n - b_{n+1}\tilde{v}_{n+1}\tilde{\psi}_{n+1}\right)^2 \mathrm{d}\zeta_n \end{aligned} \tag{3.53}$$

with $\tilde{v}_{N+1} = \tilde{\psi}_{N+1} = 0$. The outer solution of the first harmonic, $\tilde{v}_1$ and $\tilde{\psi}_1$, is in the interior region and therefore is not discussed here. The last term of (3.53) is the dissipation in the mean flow and by design through (3.49) is supposed concentrated in the innermost Nth layer. Hence essentially, this term is just

$$E^{2a-1+r_N}\int_0^\infty \left(\hat{\Gamma} - b_N\hat{v}_N\hat{\psi}_N\right)^2 \mathrm{d}\zeta_N \tag{3.54}$$

although we need to retain the full sum to derive the Euler–Lagrange equations. The full functional (3.53) will be minimized as a function of the variables r_n, p_n, e_n and s_n when the minimum of the E-exponents is a maximum. This occurs when all are made equal which essentially means that we have an equipartition of dissipation across the layers in the fluctuation field together with the mean flow dissipation in the innermost boundary layer. The conditions for this to occur are

$$\begin{aligned} 2a-1+r_N &= 1-2p_N-r_N = 1-2p_{N-1}-r_{N-1} = \ldots = 1-2p_1-r_1, \\ &= 1+2a+2p_N+2e_N-3r_N = \ldots = 1+2a+2p_1+2e_1-3r_1, \\ &= 1-2s_N-2e_N+r_{N-1} = \ldots = 1-2s_2-2e_2+r_1, \\ &= 1+2a+2s_N-2e_N+r_{N-1} = \ldots = 1+2a+2s_2-2e_2+r_1. \end{aligned} \tag{3.55}$$

Since both the size of the outermost boundary layer, $r_1 = \alpha$, and the magnitude of $\mathscr{D}_{bl} = O(E^{2a-1+r_N})$ will be determined by the coupling to the interior, the solution is parameterized by a and α as follows:

$$\left.\begin{aligned} r_n = \frac{2-a-2\alpha}{2-4^{-N+1}}\left(1-4^{-n+1}\right)+\alpha, \quad 2p_n = \frac{2-a-2\alpha}{2-4^{-N+1}}4^{-n+1}-a, \quad s_n = -\tfrac{1}{2}a, \\ 2e_n = \frac{4-2a-2\alpha 4^{-N+1}}{2-4^{-N+1}} - \frac{2-a-2\alpha}{2-4^{-N+1}}4^{-n+2}. \end{aligned}\right\} \tag{3.56}$$

To find the transverse (axial) wavelengths and structure within these layers we solve the Euler–Lagrange equations associated with minimizing (3.53). In contrast to Busse's (1970) formulation, no equations are needed here for $\tilde{v}_1$ or $\tilde{\psi}_1$ since these velocity fields are outside the domain of $\mathscr{D}_{bl}$. The equations are

$$\left.\begin{aligned} \frac{1}{b_n}\hat{\psi}_n^{\mathrm{iv}} - E^{r_n-r_N}\left(\hat{\Gamma} - b_n\hat{v}_n\hat{\psi}_n - b_{n+1}\tilde{v}_{n+1}\tilde{\psi}_{n+1}\right)\hat{v}_n = 0, \\ \frac{1}{b_n}\hat{v}_n'' + E^{r_n-r_N}\left(\hat{\Gamma} - b_n\hat{v}_n\hat{\psi}_n - b_{n+1}\tilde{v}_{n+1}\tilde{\psi}_{n+1}\right)\hat{\psi}_n = 0, \end{aligned}\right\} \quad (n=1,\ldots,N), \tag{3.57}$$

$$\left.\begin{aligned} b_{n+1}^3\tilde{\psi}_{n+1} - E^{r_n-r_N}\left(\hat{\Gamma} - b_n\hat{v}_n\hat{\psi}_n - b_{n+1}\tilde{v}_{n+1}\tilde{\psi}_{n+1}\right)\tilde{v}_{n+1} = 0, \\ b_{n+1}\tilde{v}_{n+1} - E^{r_n-r_N}\left(\hat{\Gamma} - b_n\hat{v}_n\hat{\psi}_n - b_{n+1}\tilde{v}_{n+1}\tilde{\psi}_{n+1}\right)\tilde{\psi}_{n+1} = 0, \end{aligned}\right\} \quad (n=1,\ldots,N-1) \tag{3.58}$$

which are, with the associations $w_n = b_n\psi_n$, $\theta_n = v_n$ and $h_0 = \hat{\Gamma}$, exactly Busse's (1970) equations (22) (corrected) and (23).

Consider the situation in the first $N-1$ layers. Provided that $\tilde{\psi}_{n+1}$ and $\tilde{v}_{n+1}$ are non-zero, that is we are in the inner part of the nth boundary layer, (3.58) implies that

$$b_{n+1}^2 = E^{r_n-r_N}\left(\hat{\Gamma} - b_n\hat{v}_n\hat{\psi}_n - b_{n+1}\tilde{v}_{n+1}\tilde{\psi}_{n+1}\right), \quad \tilde{v}_{n+1} = b_{n+1}\tilde{\psi}_{n+1}. \tag{3.59}$$

This may be used to describe the inner regime in which $\hat{v}_n$ and $\hat{\psi}_n$ grow from zero until $\hat{\Gamma} - b_n\hat{v}_n\hat{\psi}_n = b_{n+1}\tilde{v}_{n+1}\tilde{\psi}_{n+1} \approx 0$. Thereafter (3.59) does not hold but now $\hat{\Gamma} = b_n\hat{v}_n\hat{\psi}_n$. Resolution of the boundary layer structure is then a case of solving the dual regime problem

$$\hat{\Omega}^{\mathrm{iv}} - G\hat{\Theta} = 0, \quad \hat{\Theta}'' + G\hat{\Omega} = 0, \tag{3.60}$$

where the variables have been changed to

$$\xi = (b_{n+1}^2 b_n)^{-1/3}\zeta_n, \quad \hat{\Omega} = (b_{n+1}b_n^2)^{1/3}\hat{\Gamma}^{-1/2}\hat{\psi}_n, \quad \hat{\Theta} = (b_{n+1}/b_n)^{-1/3}\hat{\Gamma}^{-1/2}\hat{v}_n, \tag{3.61}$$

and

$$G = E^{r_n - r_N}\left(\widehat{\Gamma} - b_n\widehat{v}_n\widehat{\psi}_n - b_{n+1}\widetilde{v}_{n+1}\widetilde{\psi}_{n+1}\right)/b_{n+1}^2 \tag{3.62}$$

is 1 ($\widehat{\Omega}\widehat{\Theta}$ unspecified) for $0 \leqslant \xi \leqslant \xi^*$ and $\widehat{\Omega}\widehat{\Theta} = 1$ (G unspecified) for $\xi^* \leqslant \xi < \infty$ (Kerswell & Soward 1996). The boundary conditions are that $\widehat{\Omega} = \widehat{\Omega}' = \widehat{\Theta} = 0$ at $\xi = 0$, $\widehat{\Omega}' \to$ const as $\xi \to \infty$, together with the matching conditions at $\xi = \xi^*$ that $\widehat{\Theta}, \widehat{\Theta}', \widehat{\Omega}, \widehat{\Omega}', \widehat{\Omega}''$ and $\widehat{\Omega}'''$ are continuous, $\widehat{\Omega}\widehat{\Theta} = 1$ and $(\widehat{\Omega}\widehat{\Theta})' = 0$. The integral results

$$\beta = \int_0^\infty \widehat{\Omega}''^2\,\mathrm{d}\xi = \int_0^\infty \widehat{\Theta}'^2\,\mathrm{d}\xi = \tfrac{1}{3}\int_0^\infty G\,\mathrm{d}\xi = \tfrac{1}{2}\int_0^\infty (1 - \widehat{\Omega}\widehat{\Theta})\mathrm{d}\xi \approx 0.624 \tag{3.63}$$

then follow (Busse 1969*b*, 1978).

In the Nth layer where $\widetilde{\psi}_{N+1} = \widetilde{v}_{N+1} = 0$, the change of variables

$$\xi = \left(\widehat{\Gamma} b_N\right)^{1/3}\zeta_N, \quad \Omega = \left(\widehat{\Gamma}/b_N^2\right)^{-1/3}\widehat{\psi}_N, \quad \Theta = \left(\widehat{\Gamma}^2/b_N\right)^{-1/3}\widehat{v}_N, \tag{3.64}$$

leads to the equations

$$\Omega^{\mathrm{iv}} - (1 - \Omega\Theta)\Theta = 0, \quad \Theta'' + (1 - \Omega\Theta)\Omega = 0, \tag{3.65}$$

with boundary conditions $\Omega = \Omega' = \Theta = 0$ at $\xi = 0$, $\Theta \to 0$ and $\Omega\Theta \to 1$ as $\xi \to \infty$. This problem was first solved by Howard (1963) in his 'single'-α analysis with the results

$$\sigma = \int_0^\infty \Omega''^2\mathrm{d}\xi = \int_0^\infty \Theta'^2\mathrm{d}\xi = \tfrac{1}{5}\int_0^\infty (1-\Omega\Theta)\mathrm{d}\xi = \tfrac{1}{4}\int_0^\infty (1-\Omega\Theta)^2\mathrm{d}\xi \approx 0.337. \tag{3.66}$$

With the integral identities (3.63) and (3.66), $\mathscr{D}_{bl}$ may now be reduced to an expression in just the axial wavelengths and the two constants β and σ:

$$\mathscr{D}_{bl} = 12\pi\beta E^{2a-1+r_N}\,\widehat{\Gamma}\sum_{n=1}^{N}\left(\frac{b_{n+1}^4}{b_n}\right)^{1/3} \tag{3.67}$$

where the definition

$$b_{N+1}^{4/3} = \frac{\sigma}{\beta}\,\widehat{\Gamma}^{2/3} \tag{3.68}$$

has been made for convenience. The jump in V across the boundary layers is

$$\Delta V = \sum_{n=1}^{N} E^{a-1+r_n}\int_0^\infty \mathrm{d}\zeta_n(\widehat{\Gamma} - b_n\widehat{v}_n\widehat{\psi}_n - b_{n+1}\widetilde{v}_{n+1}\widetilde{\psi}_{n+1}) = \sum_{1}^{N}\Delta_n V. \tag{3.69}$$

Use of (3.57), (3.58) and the realization that to leading order $\widehat{\Gamma} \approx b_n\widehat{v}_n\widehat{\psi}_n + b_{n+1}\widetilde{v}_{n+1}\widetilde{\psi}_{n+1}$ for all but the innermost layer, leads to the expression

$$\Delta_n V = E^{a-1+r_N}\widehat{\Gamma}^{-1}\int_0^\infty \widehat{\psi}_n''^2 + b_{n+1}^4\widetilde{\psi}_{n+1}^2\,\mathrm{d}\zeta_n = 3\beta\left(\frac{b_{n+1}^4}{b_n}\right)^{1/3} \quad (n = 1, \ldots, N-1).$$

The jump $\Delta_N V$ across the innermost layer follows directly from the third integral in (3.66), giving the total jump as

$$\Delta V = E^{a-1+r_N}\left\{\sum_{n=1}^{N} 3\beta\left(\frac{b_{n+1}^4}{b_n}\right)^{1/3} + 2\sigma\left(\frac{\widehat{\Gamma}^2}{b_N}\right)^{1/3}\right\}, \tag{3.70}$$

after use of (3.68). Hence

$$\Delta V = O\left[\frac{\mathscr{D}_{bl}}{\mathscr{D}} = E^{a-1+r_N}\, 6\beta \sum_{n=1}^{N} \left(\frac{b_{n+1}^4}{b_n}\right)^{1/3}\right]. \tag{3.71}$$

The expression for $\mathscr{D}_{bl}$ is minimized when the axial wavelengths satisfy the recurrence relation

$$4^3 \frac{b_n^4}{b_{n-1}} = \frac{b_{n+1}^4}{b_n} \qquad (n = 2, \ldots, N). \tag{3.72}$$

In contrast to Busse (1970), there is one less equation to solve owing to the interior being a separate regime. As a result, the outermost wavelength b_1 parameterizes the solution as follows:

$$b_n = 4^{n-1}\left[4^{-N}\left(\frac{\sigma}{\beta}\right)^{3/4} \widehat{\Gamma}^{1/2}\right]^{(1-4^{1-n})/(1-4^{-N})} b_1^{(4^{1-n}-4^{-N})/(1-4^{-N})}. \tag{3.73}$$

The boundary regime dissipation is then

$$\mathscr{D}_{bl} = 4^{7/3}\pi E^{2a-1+r_N}\beta\,\widehat{\Gamma}(4^N - 1)\left[4^{-N}\left(\frac{\sigma}{\beta}\right)^{3/4} \widehat{\Gamma}^{1/2}\right]^{1/(1-4^{-N})} b_1^{-4^{-N}/(1-4^{-N})}. \tag{3.74}$$

The order of this depends on the outermost boundary layer scaling $r_1 = \alpha$ and a, the scaling of the total dissipation, whereas the exact magnitude is determined by the outermost axial wavelength b_1. The values of these unknowns will be specified by coupling to the interior flow.

3.3.2. *Interior regime*

The fluctuating velocity field in the interior matches onto the first (outermost) harmonic in the boundary layer regime. As a result, we adopt the representation

$$\tilde{\boldsymbol{u}}_i = \nabla\times\left[\frac{\sqrt{2}\,\tilde{\psi}_1 \sin(\alpha_1 z)}{s}\widehat{\boldsymbol{\phi}}\right] + \sqrt{2}\,\tilde{v}_1 \cos(\alpha_1 z)\widehat{\boldsymbol{\phi}} \tag{3.75}$$

where $\alpha_1 \gg 1$ for all cases of interest. In fact, the magnitude of $E\alpha_1^2$ is pivotal in what follows so it is worth introducing $\epsilon = O(E\alpha_1^2) = E^{1-2e_1}$ so that

$$E\alpha_1^2 = \epsilon b_1^2. \tag{3.76}$$

The leading-order interior equations can then be rewritten as

$$\Omega\,[(1+\mu)s + 2\mu V_i] = \mu E\left(\nabla^2 - \frac{1}{s^2}\right) W_i, \tag{3.77}$$

$$\frac{\alpha_1}{s}\tilde{\psi}_1\left[s\frac{\mathrm{d}}{\mathrm{d}s}\left(\frac{V_i}{s}\right)\right] = \epsilon b_1^2 \tilde{v}_1, \tag{3.78}$$

$$\tilde{v}_1\left[s\frac{\mathrm{d}}{\mathrm{d}s}\left(\frac{V_i}{s}\right)\right] = \epsilon b_1^2 \frac{\alpha_1}{s}\tilde{\psi}_1, \tag{3.79}$$

$$\Omega W_i = \frac{1}{s^2}\frac{\mathrm{d}}{\mathrm{d}s}(-s\alpha_1 \tilde{v}_1 \tilde{\psi}_1). \tag{3.80}$$

To allow compatibility with the boundary regime in which v_1 and $\alpha_1\psi_1/s$ both emerge equal to $(\Gamma/s^2)^{1/2}$, the solution

$$\alpha_1\frac{\widetilde{\psi}_1}{s}=\widetilde{v}_1,\quad V_i=-s\Delta V+\epsilon b_1^2\, s\ln s \tag{3.81}$$

must be chosen to the equations (3.78) and (3.79); recall that ΔV is the jump in V across the boundary layers, i.e. $V(1)-V_i(1)$. With this, we may integrate the remaining equations (3.77) and (3.80) for W_i and $\widetilde{v}_1$. Matching to the outermost boundary layer requires that $\widetilde{v}_1=\alpha_1\widetilde{\psi}_1/s=(\Gamma/s^2)^{1/2}$ and $\widetilde{\psi}_1'=0$ at $s=1$. The latter condition is implicitly satisfied through (3.80) as $W_i(1)=0$ so that only the former needs to be imposed, thus determining ΔV as

$$\Delta V=\frac{1+\mu}{2\mu}-48\frac{E\Gamma}{\Omega^2}-\frac{5}{12}\epsilon b_1^2 \tag{3.82}$$

and the solution

$$\Omega W_i=-12\Gamma s(1-s^2)+\frac{1}{12}\frac{\Omega^2}{E}\epsilon b_1^2\left\{3s^3\ln s+s(1-s^2)\right\}, \tag{3.83}$$

$$\widetilde{v}_1^2=\Gamma s^2(3-2s^2)+\frac{1}{48}\frac{\Omega^2}{E}\epsilon\, b_1^2 s^2\left(s^2-2s^2\ln s-1\right). \tag{3.84}$$

Notice that the expression for $\widetilde{v}_1^2$ is only positive semi-definite over $s\in[0,1]$ if

$$\frac{E\Gamma}{\Omega^2}\geqslant\frac{1}{144}\epsilon b_1^2. \tag{3.85}$$

The dissipation in the fluctuating field is

$$\mathscr{D}_{v\psi}\approx 2\pi E\int_0^1 s\mathrm{d}s\,\left\{2\alpha_1^2\widetilde{v}_1^2\right\}=\frac{5\pi}{3}\epsilon b_1^2\Gamma-\frac{\pi}{432}\frac{\Omega^2}{E}(\epsilon b_1^2)^2 \tag{3.86}$$

and in the forced field W_i,

$$\mathscr{D}_W=E\int_0^{2\pi}\mathrm{d}\phi\int_0^1 s\mathrm{d}s\left\{W_i'^2+\frac{W_i^2}{s^2}\right\}\cos^2\phi=96\pi\frac{E\Gamma^2}{\Omega^2}+\frac{\pi}{432}\frac{\Omega^2}{E}(\epsilon b_1^2)^2. \tag{3.87}$$

The total dissipation is then

$$\mathscr{D}=\mathscr{D}_{v\psi}+\mathscr{D}_W+\mathscr{D}_{bl} \tag{3.88}$$

where the dissipation associated with W_b has been neglected (see Appendix C). The character of the dominant balance in (3.88) depends on whether Ω^2/E is much greater or much less than $E^{4^{-N}}$.

3.3.3. *Supercritical case:* $\Omega^2/E\gg E^{4^{-N}}$

This is the more important case since the laminar flow is unstable when $\Omega=O(E^{1/2})$ by analogy to known results for a precessing spheroid (Kerswell 1993). Given

$$\frac{\Omega^2}{E}=E^{\gamma},\quad \gamma<4^{-N}, \tag{3.89}$$

there is only one scaling consistent with maximizing the total dissipation $\mathscr{D}$ subject to the constraint (3.85). In this, the boundary layer dissipation dominates the interior dissipation,

$$\mathscr{D}=\mathscr{D}_{bl}\gg\mathscr{D}_W+\mathscr{D}_{v\psi}\Longleftrightarrow a=2a-1+r_N \tag{3.90}$$

and

$$\frac{E\Gamma}{\Omega^2} = O(\epsilon) \Longleftrightarrow a - \gamma = 1 - 2e_1. \tag{3.91}$$

The latter is forced by the maximization process over b_1; $\mathscr{D}_{bl}$ and, hence $\mathscr{D}$, increases with b_1 until equality is obtained in (3.85) (see below). These two relations are now sufficient to specify the outermost boundary layer scaling and the order of the dissipation as follows:

$$\alpha = 1 - \frac{4^{N-1}(1-\gamma)}{4^N - 1}, \quad a = \frac{1-\gamma}{4^N - 1}. \tag{3.92}$$

With these scalings,

$$\epsilon = E^{(4^{-N}-\gamma)/(1-4^{-N})} \ll 1, \quad \alpha_1 = O\left(E^{(2.4^{-N}-1-\gamma)/[2(4^{-N}-1)]}\right) \tag{3.93}$$

and

$$\mathscr{D} = \mathscr{D}_{bl} = O\left(E^{(1-\gamma)/(4^N-1)}\right) \tag{3.94}$$

For (3.78) and (3.79) to be valid leading-order approximations, we need $\alpha_1 \gg 1$ or $\gamma > 2.4^{-N} - 1$ which effectively means $\Omega = o(1)$.

Using (3.74), the statement $\mathscr{D} = \mathscr{D}_{bl}$ can be rewritten as

$$\widehat{\Gamma} = \frac{(\beta/\sigma)^{3/2}}{[2\beta 4^{4/3}(1-4^{-N})]^2}\left[2\beta 4^{4/3}(4^N-1)b_1\right]^{2.4^{-N}}, \tag{3.95}$$

which must now be maximized over b_1, the axial wavelength in the outermost boundary layer. The restriction (3.85) means that maximum $\widehat{\Gamma}$,

$$\widehat{\Gamma}_{max} = \frac{\left[\left(3.4^{N+1}\right)^{2.4^{-N}}(\beta/\sigma)^{3/2}\right]^{1/(1-4^{-N})}}{\left[2\beta 4^{4/3}(1-4^{-N})\right]^2}, \tag{3.96}$$

is achieved at $b_1^2 = 144\widehat{\Gamma}$. The total maximal dissipation associated with an N-boundary layer solution to the variational problem for the case $\Omega^2/E = E^{\gamma}$ is then

$$\mathscr{D} = 2\pi\frac{\left[\left(3.4^{N+1}\right)^{2.4^{-N}}(\beta/\sigma)^{3/2}\right]^{1/(1-4^{-N})}}{\left[2\beta 4^{4/3}(1-4^{-N})\right]^2}E^{(1-\gamma)/(4^N-1)}. \tag{3.97}$$

Clearly in the asymptotic limit of small E, this maximum dissipation increases with N until it is ultimately independent of E, or in other words, the fluid's viscosity. Formally, the limit $N \to \infty$ in which

$$\mathscr{D} \to 2\pi\,\sigma^{-3/2}\beta^{-1/2}4^{-11/3} \approx 0.080\pi \tag{3.98}$$

cannot be reached within the framework of our asymptotic analysis owing primarily to the failure of scale separation between successive boundary layers in this limit (see Kerswell & Soward 1996 for further discussion). However, the speed with which this limit is approached as N increases is highly suggestive of its validity. Moreover, an alternative but no more defensible procedure suggested by Busse reproduces exactly the result (3.98). The asymptotic approach used to derive the expression (3.97) relies upon the fact that E is small and independent of N. Nevertheless, given the result (3.97), the question "What is the optimum choice of N at a given small finite value

of E which maximizes $\mathscr{D}$?" is irresistible. The answer is given by the expression

$$4^{-N_{opt}} = 12(\beta/\sigma)^{3/4} E^{(1-\gamma)/2} \tag{3.99}$$

which reproduces the dissipation result (3.98) at small E.

Finally, μ may be determined either directly from (3.41) as

$$\mu = \frac{b_N^{1/3}}{4\sigma \widehat{\Gamma}^{2/3}} \tag{3.100}$$

or, more simply, through a consistency condition on the jump in V across the boundary layers. When $\mathscr{D} = \mathscr{D}_{bl}$ to leading order, (3.70), (3.71) and (3.82) imply that

$$\Delta V = \tfrac{1}{2} + 2\sigma \left(\frac{\widehat{\Gamma}^2}{b_N} \right)^{1/3} = \frac{1+\mu}{2\mu} + O(\epsilon), \tag{3.101}$$

which reproduces the same $O(1)$ result for μ.

3.3.4. *Subcritical case:* $\Omega^2/E \ll E^{4^{-N}}$

Here we again take

$$\frac{\Omega^2}{E} = E^{\gamma}, \quad \text{but now} \quad \gamma > 4^{-N}.$$

In contrast to the previous case, the boundary layer dissipation does not contribute at leading order to the total dissipation in this parameter range. In fact the only consistent balance has

$$\mathscr{D} = \mathscr{D}_W \gg \mathscr{D}_{v\psi}, \mathscr{D}_{bl} \Longleftrightarrow a = \gamma \tag{3.102}$$

and

$$\mathscr{D}_{bl} = O(\mathscr{D}_{v\psi}) = O(\epsilon \Gamma) \Longleftrightarrow 2a - 1 + r_N = a + 1 - 2e_1. \tag{3.103}$$

These two relations then complete the scaling specification of the boundary layers:

$$\alpha = \frac{3(2-\gamma)}{4(2-4^{-N})}, \quad \epsilon = E^{(\gamma-4^{-N})/(2-4^{-N})}, \quad \alpha_1 = O\left(E^{(\gamma-2)/[2(2-4^{-N})]}\right), \quad \mathscr{D} = O\left(\frac{\Omega^2}{E} = E^{\gamma}\right). \tag{3.104}$$

We search for a consistent solution to (3.77)–(3.80) and (3.41) in the form

$$\left.\begin{aligned} W_i &= \frac{\Omega}{E}\left[W_i^{(0)} + \epsilon W_i^{(1)} + \ldots, \quad V_i = V_i^{(0)} + \epsilon V_i^{(1)} + \ldots, \right. \\ \widetilde{v}_1^2 &= \frac{\Omega^2}{E}\left[\widetilde{v}_1^{2(0)} + \epsilon \widetilde{v}_1^{2(1)} + \ldots, \quad \mu = \mu^{(0)} + \epsilon \mu^{(1)} + \ldots, \right. \\ \mathscr{D}/2\pi = \Gamma &= \frac{\Omega^2}{E}\left[\widehat{\Gamma}^{(0)} + \epsilon \widehat{\Gamma}^{(1)} + \ldots. \right. \end{aligned}\right\} \tag{3.105}$$

where

$$\mathscr{D}_W = \frac{\Omega^2}{E}\left[\mathscr{D}_W^{(0)} + \epsilon \mathscr{D}_W^{(1)} + \ldots, \quad \mathscr{D}_{v\psi} = \frac{\Omega^2}{E}\left[\epsilon \mathscr{D}_{v\psi}^{(1)} + \ldots, \quad \mathscr{D}_{bl} = \frac{\Omega^2}{E}\left[\epsilon \mathscr{D}_{bl}^{(1)} + \ldots. \right. \right. \right.$$

The leading-order equations are

$$\left.\begin{aligned} \frac{1+\mu^{(0)}}{\mu^{(0)}}s &= \left(\nabla^2 - \frac{1}{s^2}\right) W_i^{(0)}, \quad W_i^{(0)}(1) = 0, \\ W_i^{(0)} &= \frac{1}{s^2}\frac{\mathrm{d}}{\mathrm{d}s}\left(-s^2\tilde{v}_1^{2(0)}\right), \quad \tilde{v}_1^{2(0)}(1) = \hat{\Gamma}^{(0)}, \\ (1-\mu^{(0)})\hat{\Gamma}^{(0)} &= 0, \qquad\qquad 2\pi\hat{\Gamma}^{(0)} = \mathscr{D}_W^{(0)} \end{aligned}\right\} \tag{3.106}$$

with solution

$$\left.\begin{aligned} 2\pi\hat{\Gamma}^{(0)} = \mathscr{D}_W^{(0)} = \frac{2\pi}{48}, \quad \mu^{(0)} = 1, \quad W_i^{(0)} = \tfrac{1}{4}s(s^2-1), \\ V_i^{(0)} = 0, \quad \tilde{v}_1^{2(0)} = \tfrac{1}{48}s^2(3-2s^2). \end{aligned}\right\} \tag{3.107}$$

Working to next order,

$$2\pi\hat{\Gamma}^{(1)} = \mathscr{D}_W^{(1)} + \mathscr{D}_{v\psi}^{(1)} + \mathscr{D}_{bl}^{(1)}, \tag{3.108}$$

and from (3.81)

$$V_i^{(1)} = b_1^2 s\ln s - s\Delta, \tag{3.109}$$

where $\Delta V = \epsilon\Delta$ since $\mathscr{D}_{bl} = O(\epsilon\mathscr{D})$. Explicit evaluation of $\mathscr{D}_W^{(1)}$ can be avoided by realizing that for our purposes

$$\begin{aligned} -\left\langle V\left\{E\left(\nabla^2 - \frac{1}{s^2}\right)V + \Omega W\right\}\right\rangle &= \left\langle -\tilde{v}_1^{2(0)} s\frac{\mathrm{d}}{\mathrm{d}s}\left(\frac{V_i}{s}\right)\right\rangle \\ &\quad + \left\langle\left\{Es\frac{\mathrm{d}}{\mathrm{d}s}\left(\frac{V_b}{s}\right) - \frac{\Gamma}{s^2}\right\} s\frac{\mathrm{d}}{\mathrm{d}s}\left(\frac{V_b}{s}\right)\right\rangle \end{aligned} \tag{3.110}$$

since each side equals $\langle\widetilde{\tilde{u}_s\tilde{u}_\phi}s(\mathrm{d}/\mathrm{d}s)(V/s)\rangle$ to $O(\epsilon)$. This simplifies to

$$2\pi\hat{\Gamma}^{(0)}(2\Delta + \mu_1) = \mathscr{D}_{v\psi}^{(1)} + 2\mathscr{D}_{bl}^{(1)}. \tag{3.111}$$

Multiplying the second-order version of (3.77) by $W_i^{(0)}$ and integrating over the interior gives

$$-\mathscr{D}_W^{(1)} = 2\pi\int_0^1 s\mathrm{d}s\, W_i^{(0)}\left(\nabla^2 - \frac{1}{s^2}\right)W_i^{(1)} = 2\pi\hat{\Gamma}^{(0)}(2\Delta+\mu_1) + \mathscr{D}_{v\psi}^{(1)}, \tag{3.112}$$

so that $\mathscr{D}_W^{(1)} = -2\mathscr{D}_{v\psi}^{(1)} - 2\mathscr{D}_{bl}^{(1)}$ and hence

$$2\pi\hat{\Gamma}^{(1)} = -\mathscr{D}_{v\psi}^{(1)} - \mathscr{D}_{bl}^{(1)} \tag{3.113}$$

which is strictly negative as it should be. To complete the solution at this order, only b_1 remains to be specified and this is achieved by maximizing $\hat{\Gamma}^{(1)}$. With the constants A and B defined as follows (equation (3.74)):

$$\mathscr{D}_{bl}^{(1)} = 4^{7/3}\pi\beta\,\hat{\Gamma}^{(0)}(4^N-1)\left[4^{-N}\left(\frac{\sigma}{\beta}\right)^{3/4}\left(\hat{\Gamma}^{(0)}\right)^{1/2}\right]^{1/(1-4^{-N})} b_1^{-4^{-N}/(1-4^{-N})} = A\,b_1^{-4^{-N}/(1-4^{-N})},$$

and

$$\mathscr{D}_{v\psi}^{(1)} = \frac{5\pi}{144}b_1^2 = B\,b_1^2,$$

this maximum is

$$2\pi\widehat{\Gamma}^{(1)} = -\left[\frac{A}{2}\right]^{2(1-4^{-N})/(2-4^{-N})}\left[\frac{B(1-4^{-N})}{4^{-N}}\right]^{4^{-N}/(2-4^{-N})}\left(\frac{2-4^{-N}}{1-4^{-N}}\right) \tag{3.114}$$

which occurs at

$$b_1 = \left[\frac{A\,4^{-N}}{2B(1-4^{-N})}\right]^{(1-4^{-N})/(2-4^{-N})}. \tag{3.115}$$

In summary, we have found that when

$$\frac{\Omega^2}{E} = E^{\gamma} \ll E^{4^{-N}}$$

the upper bound on the total dissipation is

$$\mathscr{D} = 2\pi\frac{\Omega^2}{E}\left(\frac{1}{48} + \epsilon\widehat{\Gamma}^{(1)} + o(\epsilon)\right)$$

where $\widehat{\Gamma}^{(1)} < 0$ is as in (3.114) and ϵ is defined in (3.104). Hence, despite treating a considerably more constrained optimal problem here, the extremal is essentially the same as the simple Stokes result derived in §3.1!

4. Discussion

4.1. *Results summary*

We first bring together the mathematical results derived in this paper. For a fluid-filled spheroid with boundary

$$x^2 + y^2 + \frac{z^2}{c^2} = 1$$

spinning at $\widehat{\boldsymbol{k}}$ about its axis of symmetry which itself is rotating at $\boldsymbol{\Omega}$ (perpendicular to $\widehat{\boldsymbol{k}}$) in inertial space, the viscous dissipation rate $\mathscr{D}$ (in non-dimensional units of $\rho R^5\omega^3$ where ρ is the fluid density, R the equatorial radius and ω the basic container spin rate) satisfies the Stokes upper bound (§2.1)

$$\mathscr{D} \leqslant \frac{16\pi c^5}{105(4c^4+3c^2+3)}\frac{\Omega^2}{E}, \qquad \forall\Omega, E. \tag{4.1}$$

A bound independent of the fluid's viscosity E and precession rate Ω was developed in §2.5 based upon the background technique pioneered by Doering & Constantin (1992, 1994). For the parameter range of interest, $E \ll 1$, $\Omega \ll E^{-1/2}$, and $c \approx 1$, this is

$$\mathscr{D} \leqslant 0.137\pi = 0.43. \tag{4.2}$$

For a long precessing cylinder, the analogous results to (4.1) and (4.2) are (§3.1 and §3.2)

$$\mathscr{D} \leqslant \frac{\pi}{24}\frac{\Omega^2}{E}, \qquad \forall\Omega, E. \tag{4.3}$$

and

$$\mathscr{D} \leqslant 0.103\pi = 0.32, \tag{4.4}$$

where now the dissipation rate is per unit length in the axial direction. In this geometry, the Howard/Busse mean field formulation could also be employed to

produce a more tightly constrained optimization problem (§3.3). In the asymptotic limit of $E \to 0$, the following results were derived when $\Omega^2/E = E^\gamma$ and N is a chosen positive integer:

$$\mathscr{D} \leqslant \frac{\Omega^2}{E}\left[\frac{\pi}{24} - O\left(E^{(\gamma-4^{-N})/(2-4^{-N})}\right) + \ldots\right], \tag{4.5}$$

valid for

$$4^{-N} < \gamma < (18+4^{1-N})/13 \iff E^{(31+4^{1-N})/26} \ll \Omega \ll E^{(1+4^{-N})/2}$$

and

$$\mathscr{D} \leqslant 2\pi \frac{\left[\left(3.4^{N+1}\right)^{2.4^{-N}}(\beta/\sigma)^{3/2}\right]^{1/(1-4^{-N})}}{\left[2\beta 4^{4/3}(1-4^{-N})\right]^2} E^{(1-\gamma)/(4^N-1)} \xrightarrow{N\uparrow\infty} 0.080\pi \tag{4.6}$$

valid for

$$-\frac{1-\frac{3}{2}\times 4^{-N}}{1-\frac{1}{2}\times 4^{-N}} < \gamma < 4^{-N} \iff E^{(1+4^{-N})/2} \ll \Omega \ll E^{4^{-N}/(2-4^{-N})}.$$

Most importantly, the tighter upper bounds, (4.5) and (4.6), exhibit the same functional dependences on E and Ω as the independently derived bounds (4.3) and (4.4). This is reassuring but certainly no guarantee that these scaling laws reflect any aspect of the true turbulent dissipation rate behaviour. However, the fact that the upper bound becomes independent of Ω and E for $O(E^{1/2}) \leqslant \Omega$ is consistent with Kolmogorov's scaling view of turbulent dissipation and previous upper bound results for unidirectional shear flow (Busse 1970; Doering & Constantin 1992, 1994) which are all independent of the fluid's viscosity. There, the driving parameter – the Reynolds number – and the fluid viscosity are one and the same so that the dissipation is then formally independent of both. Here, they differ, with the combination Ω^2/E characterizing the precessional driving and E the fluid viscosity, but a similar conclusion still appears to hold true.

As far as the numerical coefficients in the bounds are concerned, very little improvement is obtained even though the variational problem of §3.3 is substantially more constrained. Surprisingly, there is only a 20% improvement in the upper bound (4.4), and essentially none in the Stokes bound (4.3). Although disheartening in the sense that improvement is so minimal, this does indicate that the upper bounds, (4.1) and (4.2), derived for the oblate spheroidal case are likely to be 'good' in the sense that they probably cannot be lowered in any significant way.

More generally, the relative performance of the 'background' technique against the more involved Howard/Busse formalism is unexpectedly good. It remains to be seen whether this can be relied upon in other shear flow and convection problems†. Upper bounds published to date using this method (Doering & Constantin 1992, 1994, 1996; Constantin & Doering 1995; Gebhardt *et al.* 1995) have relied on very simple but necessarily conservative functional arguments such as those used in the first half of §2.5 to circumvent the spectral constraint. Consequently, there is considerable room for improvement in these bounds, as illustrated by the second half of §2.5. This is an ongoing area of investigation (C. R. Doering, private communication).

4.2. *Experimental data*

The first and still most striking data showing how the viscous dissipation varies with precession rate were collected by Malkus (1968, figure 4, see also Gans 1970) using

† Note added in proof: The answer appears to be yes – see Kerswell (1996)

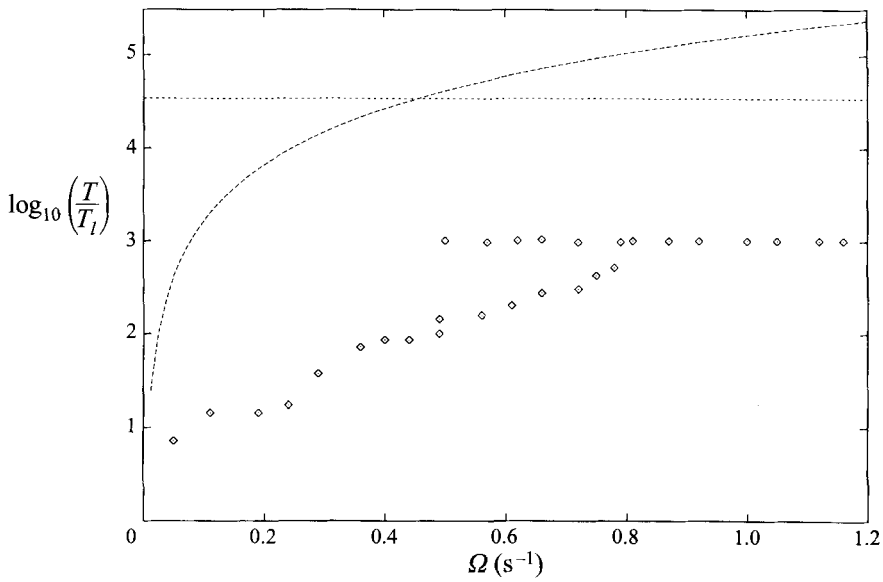

FIGURE 1. Malkus's experimental torque data T (from his figure 4, 1968) normalized by T_l, the laminar torque at $\Omega = 0.5\ \mathrm{s}^{-1}$, is replotted here using diamonds on a $\log_{10}$ scale against Ω, the dimensional precession rate ($\omega = 30\pi\ \mathrm{s}^{-1}$, $E = 1.9 \times 10^{-6}$, $c = 0.9$ and $R = 0.075$ m). The Stokes upper bound, $0.035\Omega^2/E$, (long dashed line) and background upper bound, 0.43, (short dashed line) also so normalized are shown for comparison purposes.

an oblate container with $c = 0.9$. This clearly shows the torque exhibiting hysteresis between a lower branch which evolves continuously from the initial laminar response and a constant upper branch presumably corresponding to 'saturated' turbulence. Figure 1 shows how the bounds (4.1) and (4.2) compare to these data. After the initial laminar phase where the torque varies with Ω^2, the data on the lower branch do not parallel the Stokes upper bound (4.2), seeming, if anything, to vary exponentially with Ω rather than quadratically. Intriguingly, the cross-over point between the bounds, $\Omega = 0.45\ \mathrm{s}^{-1}$, is quite close to the value at which the upper branch begins, $\Omega = 0.5\ \mathrm{s}^{-1}$. On this upper branch, the torque clearly becomes independent of the precession rate, mirroring the upper bound (4.2) which exceeds it by a factor of 34, i.e. 1.5 orders of magnitude‡. This sort of discrepancy is fairly typical in upper-bounding work (e.g. Busse 1970 who reports an order of magnitude difference between his bound and experimental data) and is construed more as a comment on the numerical coefficient in the upper bound than the correctness of its parametric scaling on E.

Later and more extensive experiments were undertaken by Vanyo (see Vanyo 1991 and Vanyo *et al.* 1995 for references) in which containers with more Earth-like oblateness ($c = 1 - \frac{1}{400}$) were of particular interest. His results were all essentially similar regardless of whether precessing spheres, spheroids, cylinders, filled or not, baffled or not were studied. The torque, and hence dissipation, would increase smoothly for small Ω, then undergo a rapid transition to a much larger value leading ultimately onto a flat plateau. Once there, the torque would then be independent of any further changes in the precession rate Ω (Vanyo 1984, p. 175). Hysteresis

‡ This is assuming the corrected value of $R = 0.075$ m for the semi-major axis rather than the 0.0375 m quoted when the factor is just $34/2^5$, and the Stokes bound is actually exceeded (W.V.R. Malkus, private communication).

was only found for sufficiently non-spherical containers, being absent, for example, in spheroidal containers with $c = 1 \pm \frac{1}{400}$ (Vanyo 1991, p. 215) and spheres (Vanyo 1984, p. 174). Unfortunately, much of the data were projected down onto a two-dimensional space (Vanyo 1991, figure 7) suggested by his 'rigid sphere' model (Vanyo & Likins 1972) and cannot be recovered for our purposes here. Nevertheless, deviances away from this rigid sphere model, which essentially proposes the dominant role of a laminar Ekman boundary layer in the dissipation, are noteworthy in that they seem to tie in with the upper bounds. At large Ekman number, Vanyo found that the Stokes dissipation result of Busse (Vanyo, Lu & Weyant 1975) matched the data well. This is none other than the Stokes upper-bound result for a sphere. More significantly at high forcing, Vanyo remarked that the dissipation became independent of the viscosity (Vanyo 1991, p. 221) to explain the eventual divergence between his model and the data.

Figure 2 of Vanyo (1984), however, does allow some direct comparisons to be made. The apparent maximum achieved torques in an oblate spheroid with $c = 1 - \frac{1}{400}$ of ≈ 0.1 Nm for $\theta = 23.5°$ and ≈ 0.02 Nm for $\theta = 10°$ are factors of 160 and 240 times smaller than the Stokes upper-bound result and 270 and 1370 times smaller than the background bound! This increased discrepancy compared to Malkus's results is clearly a direct result of the smaller oblateness of the container and points to an undoubted shortcoming of the upper bounds derived here. The flow dynamics are unquestionably sensitive to the container's oblateness whereas the upper bounds are not.

4.3. *Conclusions*

Experimental measurements of the viscous dissipation realized in highly forced precessing systems do seem to reflect the parametric scaling of the 'background' upper bound (4.2): the dissipation ultimately becomes independent of the precession rate and fluid's viscosity. At what point this occurs or at what magnitude is far less clear but certainly appears sensitive to the container's geometry. The Stokes upper bound, although holding true, does not parallel the torque variation at intermediate precession rates beyond the initially laminar response. It appears better suited to characterizing slowly spinning containers rather than the rapidly rotating cases of most geophysical interest.

The plausible picture that has emerged then, is one in which a precessing fluid system can turbulently dissipate energy at a maximal rate on the order of $\rho R^5 \omega^3$ unrelated to the precessional forcing or viscosity (ρ is the fluid density, R, a typical length scale and ω is the spin rate). Both the background method due to Doering & Constantin and the Howard/Busse formalism suggest this through optimizing solutions with intense boundary layers which dominate the dissipation. To assume that this carries over to the realized turbulent flow is reasonable but nevertheless presumptuous. Experimental observations clearly indicate the continual crashing of coherent structures to small-scale disorder throughout the bulk interior of the flow (Malkus 1968; Vanyo *et al.* 1995; Manasseh 1992, 1994) suggesting that the interior may be far from insignificant in the total dissipation budget. This inconsistency may simply be a dynamical consequence of the turbulent boundary layers absent in the variational formulations studied here. Alternatively and more profoundly, it could also be an indication that precessionally stirred turbulent flow has a more sophisticated design than to just maximize the global dissipation. In this latter scenario, we would then have no right to expect that the variational solution which optimizes the dissipation would closely resemble the realized turbulent one.

Geophysically, the precessing Earth in its most simplest terms can be considered as a precessing oblate fluid-filled spheroid with $c = 1 - \frac{1}{400}$, $\Omega = 1$ day/25 800 years $\times \sin 23.5°$ and $E \approx 10^{-15}$, with $\rho = 10^4 \text{kg m}^{-3}$, $R = 3.5 \times 10^6 \text{m}$ and $\omega = 7 \times 10^{-5}$. Non-dimensionally, this is exactly the configuration used by Vanyo (1984) but with Ω and E reduced down to 10^{-7} and 10^{-15} respectively. If, as is the suggestion, the 'saturated' turbulent dissipation is independent of both Ω and E, then a fully turbulent Earth should consume energy at a similar (non-dimensional) rate to that found in these experiments. Building in a discrepancy factor of 3 orders of magnitude as observed above relative to the 'background' upper bound, this advocates that a dissipation of 4.3×10^{-4} in non-dimensional units or $O(10^{21})$ W may potentially be realized in a fully turbulent outer core! This is fully 14 orders of magnitude more than the well-known laminar value of $O(10^7)$ W (e.g. Loper 1975). Of course, there is absolutely no observational evidence to indicate that anything like this dissipation is occurring in the outer core. In fact, an observational constraint of 10^{12} W based upon length-of-day measurements puts a strict limit on how much energy can be precessionally supplied to the Earth's core. What it does indicate, however, is the potency of precessional driving: even a weakly stirred outer core could extract sufficient energy to quench the geodynamo's estimated thirst of $10^{10}/10^{11}$ W.

Our conclusion is then a reiteration of that drawn by Roberts & Gubbins (1987): there are no reasons to dismiss the possibility of a rotationally (tidally and/or precessionally) powered dynamo on purely energetic grounds. The fundamental objection is, and remains, that it is unclear how the rapidly (daily) fluctuating precessional and tidal forcings can generate slow motions (on Ohmic diffusion timescales) in the outer core. Some recent progress has been made in this direction through the identification of the initial instability mechanism (Malkus 1989, 1994; Kerswell 1993, 1994) which operates through the pairwise excitation of inertial waves. Even though their frequencies are fast, the secular growth of the instability is on the Ohmic diffusion timescale. Nevertheless, assessing the feasibility of a rotationally powered dynamo still presents a considerable and worthy challenge even though it remains overshadowed by more plausible convective alternatives.

I am very grateful to Professor A. M. Soward for the many discussions we have shared concerning the nature of Professor F. Busse's multi-α solutions.

Appendix A

Here we look for the optimal one-dimensional background field for the spherical case. The exact spectral constraint (2.36) is intractable as it stands so the more conservative version

$$\int_0^1 r(1-r)|f'|\mathrm{d}r \leqslant E \tag{A 1}$$

is used (see equation (2.38)). Henceforth, our extremal profile is not guaranteed to be the true optimum but only a reasonable approximation to it. Furthermore, since f must decrease (monotonically) from 1 at the boundary to 0 in the interior, the constraint (A 1) forces the background field to have a boundary layer of thickness $O(E)$. This ensures that $\mathscr{G}_{min} \ll E\langle|\nabla \boldsymbol{U}|^2\rangle$ so that the upper bound to be minimized is just the background dissipation

$$E\langle|\nabla \boldsymbol{U}|^2\rangle = \tfrac{8}{3}\pi E \int_0^1 r^4 f'^2 \,\mathrm{d}r + O(E). \tag{A 2}$$

Looking ahead, the Euler–Lagrange equation to be solved does not have a regular solution at the origin. Hence we are forced to consider a solution with $f = 0$ for all radii $r \leqslant 1 - \delta$ where $\delta = O(E)$ is to be determined as part of the solution. The minimization problem is then the following:

minimize
$$\mathscr{D}_U = \tfrac{8}{3}\pi E \int_{1-\delta}^{1} r^4 f'^2 \mathrm{d}r \tag{A 3}$$

subject to
$$f(1) = 1, \quad f(1-\delta) = 0, \quad f'(1-\delta) = \mu \tag{A 4}$$

and
$$\int_{1-\delta}^{1} r(1-r) f' \mathrm{d}r = aE \tag{A 5}$$

where $0 \leqslant a \leqslant 1$ and $\mu \geqslant 0$ is a free parameter because f' need not be continuous at $r = 1 - \delta$. The Euler–Lagrange equation associated with the Lagrangian
$$\mathscr{L} = \int_{1-\delta}^{1} r^4 f'^2 \mathrm{d}r - \lambda \left\{ \int_{1-\delta}^{1} r(1-r) f' \mathrm{d}r - aE \right\} \tag{A 6}$$

is then
$$(2r^4 f')' = \lambda(1 - 2r) \tag{A 7}$$

with the solution
$$f = (1-\xi)^2 + \mu\delta\, \xi(1-\xi) + O(\delta) \tag{A 8}$$

for $0 \leqslant \xi \leqslant 1$ where
$$1 - r = \delta\xi, \quad \lambda = \frac{4(\mu\delta - 1)}{\delta^2}, \quad \mu\delta^2 + 2\delta - 6aE = 0. \tag{A 9}$$

The background dissipation is
$$\mathscr{D}_U = \frac{4\pi(8 + \mu^3\delta^3)}{27a} \tag{A 10}$$

which is minimized when $\mu = 0$ and $a = 1$ so that the spectral constraint is just satisfied. The smooth profile $f = r^{1/E}$ discussed in §2.5 has a dissipation of $4\pi/3$, exceeding the minimum (A 10) by only 12.5%.

Appendix B

In this Appendix, we solve the equations
$$\frac{\mathrm{d}f}{\mathrm{d}r}\frac{\partial}{\partial\theta}(\psi \sin\theta) + E\mathscr{F}\mathscr{D}^2 v = 0, \tag{B 1}$$

$$\frac{\mathrm{d}f}{\mathrm{d}r}\frac{\partial}{\partial\theta}(v \sin\theta) + E\mathscr{F}\mathscr{D}^4 \psi = 0, \tag{B 2}$$

where
$$\mathscr{D}^2 = \nabla^2 - \frac{1}{(r\sin\theta)^2}, \quad f(r) = r^{1/\delta},$$

with boundary conditions
$$\psi = \frac{\partial\psi}{\partial r} = v = 0|_{r=1}, \tag{B 3}$$

numerically to justify the WKB analysis used in §2.5. An eigensolution with v symmetric about the equator attains the extremal value of $\mathscr{F}$ and so we use the expansions

$$v(r,\theta) = \sum_{n=1}^{N} v_n(r) P_{2n-1}^1(\cos\theta) = \sum_{n=1}^{N}\sum_{m=1}^{M} v_{nm} T_{2m-1}(r) P_{2n-1}^1(\cos\theta),$$

$$\psi(r,\theta) = \sum_{n=1}^{N} \psi_n(r) P_{2n}^1(\cos\theta) = \sum_{n=1}^{N}\sum_{m=1}^{M} \psi_{nm} r T_{2m-1}(r) P_{2n}^1(\cos\theta)$$

where $T_m(r) = \cos(m\cos^{-1} r)$ is the mth Chebyshev polynomial, $P_n^1(\cos\theta)$ is the first order, nth degree associated Legendre function, and the parities of v and ψ with respect to r have been built in (Kerswell & Davey 1996). Following the work by Hollerbach (1994*a*, *b*), associated Legendre functions are used because the operators $\partial/\partial\theta(\sin\theta)$ and $\mathscr{D}^2$ then have the very simple action

$$\frac{\partial}{\partial\theta}(\sin\theta P_l^1(\cos\theta)) = \frac{l(l+1)}{2l+1}\left[P_{l+1}^1(\cos\theta) - P_{l-1}^1(\cos\theta)\right], \tag{B 4}$$

$$\mathscr{D}^2 g(r) P_l^1(\cos\theta) = \left(\frac{\mathrm{d}^2}{\mathrm{d}r^2} + \frac{2}{r}\frac{\mathrm{d}}{\mathrm{d}r} - \frac{l(l+1)}{r^2}\right) g(r) P_l^1(\cos\theta). \tag{B 5}$$

This means that (B 1) and (B 2) become respectively

$$\frac{\mathrm{d}f}{\mathrm{d}r}\left[\frac{2n(2n+1)}{4n+1}\psi_n - \frac{2(n-1)(2n-1)}{4n-3}\psi_{n-1}\right] = E\mathscr{F}\left[\frac{\mathrm{d}^2}{\mathrm{d}r^2} + \frac{2}{r}\frac{\mathrm{d}}{\mathrm{d}r} - \frac{2n(2n-1)}{r^2}\right] v_n, \tag{B 6}$$

$$\frac{\mathrm{d}f}{\mathrm{d}r}\left[\frac{2(n+1)(2n+1)}{4n+3}v_{n+1} - \frac{2n(2n-1)}{4n-1}v_n\right] = E\mathscr{F}\left[\frac{\mathrm{d}^2}{\mathrm{d}r^2} + \frac{2}{r}\frac{\mathrm{d}}{\mathrm{d}r} - \frac{2n(2n+1)}{r^2}\right]^2 \psi_n. \tag{B 7}$$

Collocating these over the positive zeros of $T_{2M}(r)$ gives rise to the eigenvalue problem

$$\boldsymbol{A}\boldsymbol{x} = E\mathscr{F}\boldsymbol{B}\boldsymbol{x} \tag{B 8}$$

where $\boldsymbol{x} = [v_1, \psi_1, v_2, \psi_2, v_3, \ldots]^T$, $\boldsymbol{A}$ is block tridiagonal and $\boldsymbol{B}$ is block diagonal. Forward iteration of the matrix $\boldsymbol{B}^{-1}\boldsymbol{A}$ then reveals the largest eigenvalue $\mathscr{F}$.

Figure 2 clearly shows the modulated Taylor vortex structure of the solution centred at the equator for the case of $\delta = 10^{-2}$. Figure 3 and table 1 compare the results of solving the full PDEs (B 1) and (B 2) with the WKB approach which reduces the problem to a one-dimensional eigenvalue calculation.

Appendix C

Here we examine the validity of the assumptions adopted in the main text. The main approximation is that (3.28) may be divided into simpler interior (3.38) and boundary layer (3.40) equations. In solving these equations, the boundary layer component of W, W_b, is then ignored. The boundary layer version of (3.36) is

$$\Omega(1+\mu)s + 2\mu\Omega V_b = \mu E\left(\nabla^2 - \frac{1}{s^2}\right) W_b \tag{C 1}$$

from which we can estimate that in the nth boundary layer

$$W_b = O\left(\frac{\Omega}{E}E^{2r_n}\right) = O(E^{2r_n})W_i, \quad \mathscr{D}_{W_b} = O(E^{3r_n})\mathscr{D}_{W_i}. \tag{C 2}$$

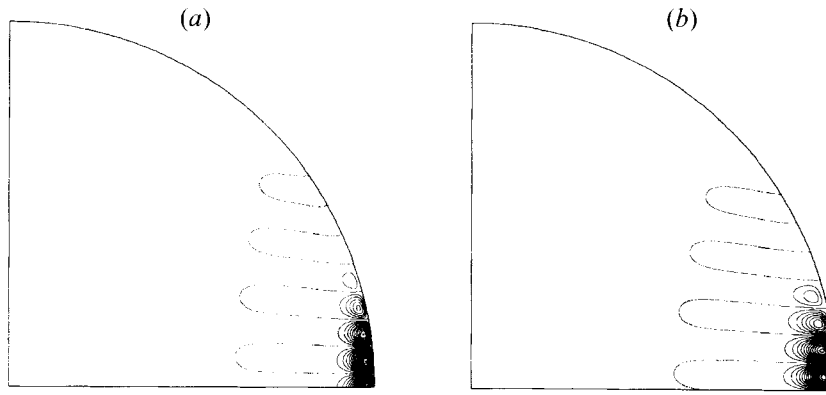

FIGURE 2. The numerically calculated modulated Taylor vortex structure is shown here clearly centred at the equator for $f(r) = r^{100}$ using a truncation level of $N = M = 100$: (*a*) corresponds to v and (*b*) to ψ (contours are at 5% intervals).

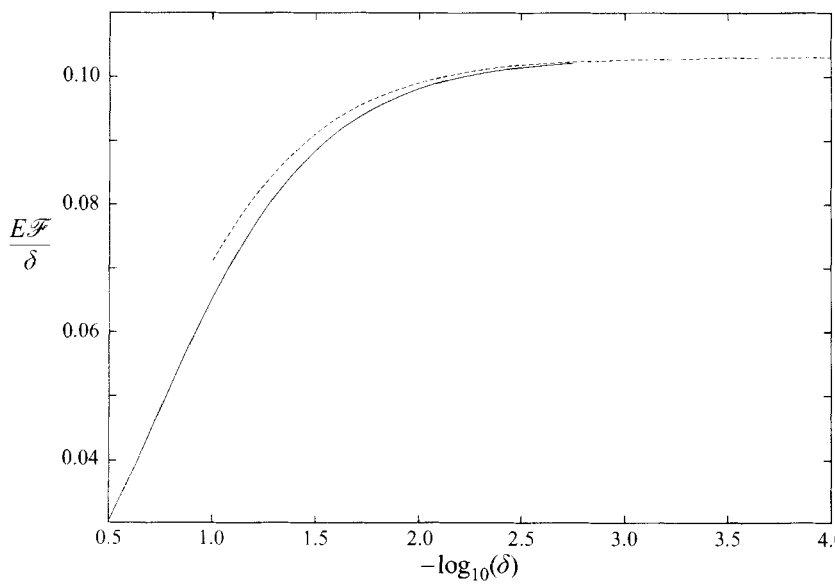

FIGURE 3. A plot of the largest eigenvalue $E\mathscr{F}/\delta$ versus $-\log_{10}(\delta)$. The solid line is the result of solving the full PDEs whereas the dashed line is the WKB estimate. The limiting value of $E\mathscr{F}/\delta \to 0.103$ as $\delta \to 0$ is used in the asymptotics of §2.5.

With this

$$\Omega W_b = O(E^{\gamma+4r_n-r_N-a})E\left(\nabla^2 - \frac{1}{s^2}\right)V_b \tag{C 3}$$

since

$$\frac{1}{s^2}(\Gamma + s^2\overline{\tilde{u}_s\tilde{u}_\phi}) = Es\frac{\mathrm{d}}{\mathrm{d}s}\left(\frac{V_b}{s}\right) = O(E^{r_N-r_n+a}).$$

Thus we need $\gamma + 4r_n - r_N - a > 0$ for $n = 1, \ldots, N$ if (3.40) is to be valid. As $r_1 = \alpha < r_2 < \ldots < r_N$, this condition reduces to

$$\gamma + 4\alpha - r_N - a > 0. \tag{C 4}$$

	Numerical	WKB	
$-\log_{10}(\delta)$	$E\mathscr{F}/\delta$	$E\mathscr{F}/\delta$	k
1	0.0653	0.0711	0.492
1.25	0.0790	0.0831	0.452
1.5	0.0885	0.0911	0.430
1.75	0.0945	0.0961	0.418
2.0	0.0981	0.0990	0.412
2.25	0.1002	0.1008	0.408
2.5	0.1014	0.1018	0.406
2.75	0.1021	0.1023	0.405
3		0.1026	0.405
3.5		0.1029	0.404
4		0.1030	0.404

TABLE 1. The results of maximising $\mathscr{F}$ at various δ using a full numerical procedure and the WKB approximation.

In the interior

$$E\left(\nabla^2 - \frac{1}{s^2}\right) V_i = O\left(\frac{E^2}{\Omega^2} V_i\right) \Omega W_i \tag{C 5}$$

so that (3.38) is only valid if $V_i = o(E^{\gamma-1})$.

For the supercritical case, $\Omega^2/E = E^\gamma \gg E^{4^{-N}}$, the most restrictive condition is (C 4) which requires

$$\gamma > -\frac{1 - \frac{3}{2} \times 4^{-N}}{1 - \frac{1}{2} \times 4^{-N}} \quad \Longrightarrow \Omega = o\left(E^{4^{-N}/(2-4^{-N})}\right). \tag{C 6}$$

Hence, by choosing N large enough, this effectively means that Ω must be $o(1)$.

In the subcritical case, $\Omega^2/E = E^\gamma \ll E^{4^{-N}}$, the first criterion broken as γ increases is that

$$\mathscr{D}_{W_b} = o(\epsilon)\mathscr{D}_{W_i} \quad \Longrightarrow \gamma < \frac{18 + 4^{1-N}}{13}, \tag{C 7}$$

which must hold if $\mathscr{D}_{W_b}$ is to be ignored in (3.108). Violation of this, however, only compromises the calculation of the higher-order correction $\widehat{\Gamma}^{(1)}$. Otherwise the only other restriction is that $\gamma < 2$ at which point the solution procedure completely fails (e.g. α_1 is no longer large). Despite this, the leading-order bound should still hold regardless since this has already been derived in §3.1 under general conditions.

REFERENCES

BUSSE, F. H. 1969*a* On Howard's upper bound for heat transport by turbulent convection. *J. Fluid Mech.* **37**, 457–477.

BUSSE, F. H. 1969*b* Bounds on the transport of mass and momentum by turbulent flow. *Z. Angew. Math. Phys.* **20**, 1–14.

BUSSE, F. H. 1970 Bounds for turbulent shear flow. *J. Fluid Mech.* **41**, 219-240.

BUSSE, F. H. 1978 The optimum theory of turbulence. *Adv. Appl. Mech.* **18**, 77–121.

CHANDRASEKHAR, S. 1961 *Hydrodynamic and Hydromagnetic Stability*. Oxford University Press.

CONSTANTIN, P. & DOERING, C. R. 1995 Variational bounds on energy-dissipation in incompressible flows: II. channel flow. *Phys. Rev.* E **51**, 3192–3198.

DOERING, C. R. & CONSTANTIN, P. 1992 Energy dissipation in shear driven turbulence. *Phys. Rev. Lett.* **69**, 1648–1651.

DOERING, C. R. & CONSTANTIN, P. 1994 Variational bounds on energy dissipation in incompressible flows: shear flow. *Phys. Rev.* E **49**, 4087–4099.

DOERING, C. R. & CONSTANTIN, P. 1996 Variational bounds on energy dissipation in incompressible flows: III. convection. *Phys. Rev.* E **53**, 5957–5981.

GANS, R. F. 1970 On the hydromagnetic precession in a cylinder. *J. Fluid Mech.* **45**, 111–130.

GEBHARDT, T., GROSSMANN, S., HOLTHAUS, M. & LÖHDEN, M. 1995 Rigorous bound on the plane-shear-flow dissipation rate. *Phys. Rev.* E **51**, 360–365.

HOLLERBACH, R. 1994*a* Imposing a magnetic field across a nonaxisymmetric shear layer in a rotating spherical shell. *Phys. Fluids* **6**, 2540–2544.

HOLLERBACH, R. 1994 *b* Magnetohydrodynamic Ekman and Stewartson layers in a rotating spherical shell. *Proc. R. Soc. Lond.* A **444**, 333–346.

HOPF, E. 1941 Ein allgemeiner endlichkeitssatz der hydrodynamik. *Mathematische Annalen* **117**, 764–775.

HOWARD, L. N. 1963 Heat transport by turbulent convection. *J. Fluid Mech.* **17**, 405–432.

HOWARD, L. N. 1972 Bounds on flow quantities. *Ann. Rev. Fluid Mech.* **4**, 473–494.

HOWARD, L. N. 1990 Limits on the transport of heat and momentum by turbulent convection with large scale flow. *Stud. Appl. Maths* **83**, 273–285.

IERLEY, G. R. & MALKUS, W. V. R. 1988 Stability bounds on turbulent Poiseuille flow. *J. Fluid Mech.* **187**, 435–449.

JOSEPH, D. D. 1976 *Stability of Fluid Motions I.* Springer.

KENNETT, R. G. 1974 Convectively-driven dynamos. *GFD Summer School Fellowship Lectures*, Woods Hole, pp. 94–117.

KERSWELL, R. R. 1993 The instability of precessing flow. *Geophys. Astrophys. Fluid Dyn.* **72**, 107–144.

KERSWELL, R. R. 1994 Tidal excitation of hydromagnetic waves and their damping in the Earth. *J. Fluid Mech.* **274**, 219–241.

KERSWELL, R. R. 1996 Variational bounds on shear driven turbulence and turbulent Boussinesq convection. Submitted to *Physica* D.

KERSWELL, R. R. & DAVEY, A. 1996 On the linear instability of elliptic pipe flow. *J. Fluid Mech.* **316**, 307–324.

KERSWELL, R. R. & SOWARD, A. M. 1996 Upper bounds for turbulent Couette flow incorporating the poloidal power constraint. *J. Fluid Mech.* (submitted).

KOBINE, J. J. 1995 Inertial wave dynamics in a rotating and precessing cylinder. *J. Fluid Mech.* **303**, 233–252.

LOPER, D. E. 1975 Torque balance and energy budget for the precessionally driven dynamo. *Phys. Earth. Planet. Inter.* **11**, 43–60.

MAHALOV, A. 1993 The instability of rotating fluid columns subjected to a weak external Coriolis field. *Phys. Fluids* **5**, 891–900.

MALKUS, W. V. R. 1954 The heat transport and spectrum of thermal turbulence. *Proc. R. Soc. Lond.* A **225**, 196–212.

MALKUS, W. V. R. 1963 Precessional torques as the cause of geomagnetism. *J. Geophys. Res.* **68**, 2871–2886.

MALKUS, W. V. R. 1968 Precession of the Earth as the cause of geomagnetism. *Science* **160**, 259–264.

MALKUS, W. V. R. 1989 An experimental study of global instabilities due to tidal (elliptical) distortion of a rotating elastic cylinder. *Geophys. Astrophys. Fluid Dyn.* **48**, 123–134.

MALKUS, W. V. R. 1994 Energy sources for planetary dynamos.In *Theory of Solar and Planetary Dynamos.* NATO ASI Conference Series, Cambridge University Press.

MALKUS, W. V. R. & SMITH, L. M. 1989 Upper bounds on functions of the dissipation rate in turbulent shear flow. *J. Fluid Mech.* **208**, 479–507.

MANASSEH, R. 1992 Breakdown regimes of inertia waves in a precessing cylinder. *J. Fluid Mech.* **243**, 261–29.

MANASSEH, R. 1994 Distortions of inertia waves in a rotating fluid cylinder forced near its fundamental mode resonance. *J. Fluid Mech.* **265**, 345–370.

PAYNE, L. & WEINBERGER, H. 1963 An exact stability bound for Navier-Stokes flow in a sphere. In *Nonlinear Problems* (ed. R. E. Langer). University of Wisconsin Press.

POINCARÉ, H. 1910 Sur la précession des corps deformable. *Bull. Astron.* **27**, 321.

PROCTOR, M. R. E. 1979 Necessary conditions for the magnetohydrodynamic dynamo. *Geophys. Astrophys. Fluid Dyn.* **14**, 127–145.

ROBERTS, P. H. & GUBBINS, D. 1987 Origin of the main field: kinematics. In *Geomagnetism*, vol. 2 (ed. J. A.Jacobs), p. 193. Academic.

ROCHESTER, M. G., JACOBS, J. A., SMYLIE, D. E. & CHONG, K. F. 1975 Can precession power the geomagnetic dynamo? *Geophys. J. R. Astron. Soc.* **43**, 661–678.

SELMI, M. & HERBERT, T. 1995 Resonance phenomena in viscous fluids inside partially filled spinning and nutating cylinders. *Phys. Fluids* **7**, 108–120.

SERRIN, J. 1959 On the stability of viscous fluid motions. *Arch. Rat. Mech. Anal.* **3**, 1–13.

SMITH, L. M. 1991 Turbulent Couette flow profiles that maximise the efficiency function. *J. Fluid Mech.* **227**, 509–525.

SOWARD, A. M. 1980 Bounds for turbulent convective dynamos. *Geophys. Astrophys. Fluid Dyn.* **15**, 317–341.

SOWARD, A. M & JONES, C. A. 1983 The linear stability of the flow in the narrow gap between two concentric rotating spheres. *Q. J. Mech. Appl. Maths* **36**, 19–42.

STACEY, F. D. 1973 The coupling of the core to the precession of the Earth. *Geophys. J. R. Astron. Soc.* **33**, 47–55.

TOOMRE, A. 1996 On the coupling of the Earth's core and the mantle during the 26,000-year precession. In *The Earth-Moon System* (ed. B. G. Marsden & A. G. W. Cameron), pp. 33–45. Plenum.

TOWNSEND, A. A. 1956 *The Structure of Turbulent Shear Flow.* Cambridge University Press.

VANYO, J. P. 1984 Earth core motions: experiments with spheroids. *Geophys. J. R. Astron. Soc.* **77**, 173–183.

VANYO, J. P. 1991 A geodynamo powered by luni-solar precession. *Geophys. Astrophys. Fluid Dyn.* **59**, 209–234.

VANYO, J. P. & LIKINS, P. W. 1972 Rigid-body approximations to turbulent motion in a liquid-filled, precessing, spherical cavity. *Trans. ASME J. Appl. Mech.* **39**, 18–24.

VANYO, J. P., LU, V. C. & WEYANT, T. F. 1975 Dimensionless energy dissipation for precessional flows in the region of $Re = 1$. *Trans. ASME J. Appl. Mech.* **42**, 881–882.

VANYO, J. P., WILDE, P., CARDIN, P. & OLSON, P. 1995 Experiments on precessing flows in the Earth's liquid core. *Geophys. J. Intl* **121**, 136–142.

WOOD, W. W. 1966 An oscillatory disturbance of rigidly rotating fluid. *Proc. R. Soc. Lond.* A **298**, 181–212.

WORTHING, R. A. 1995 Contributions to the variational theory of convection. PhD thesis, MIT.